



Confocal fluorescence microscopy of colloidal quantum dots

THESIS

submitted in partial fulfillment of the
requirements for the degree of

BACHELOR OF SCIENCE

in

PHYSICS

Author : M. van den Nieuwenhuijzen
Student ID : 2042096
Supervisor : prof. dr. M.P. van Exter
Second corrector : prof. dr. M.A.G.J. Orrit

Leiden, The Netherlands, March 10, 2021

Confocal fluorescence microscopy of colloidal quantum dots

M. van den Nieuwenhuijzen

Huygens-Kamerlingh Onnes Laboratory, Leiden University
P.O. Box 9500, 2300 RA Leiden, The Netherlands

March 10, 2021

Abstract

This thesis investigates the fluorescence properties of 605 nm and 655 nm colloidal quantum dots. Samples with different densities of both types of quantum dots were created and examined with a confocal fluorescence microscope. In particular, the thesis focuses on the spatial distribution of the quantum dots on the sample, the characteristics of their luminescence decay and the effects of blinking and bleaching.

Three different methods were used to study the former phenomena. Spatial scans of the samples helped to locate the quantum dots and revealed that they have a high tendency to cluster. Time-resolved measurements under pulsed excitation provided information on the luminescence decay and show varying, multi-exponential decay times. Finally, extended (minutes long) observation under c.w. excitation provided information on the effects of blinking and bleaching. Based on the experimental results, the thesis finally gives an advice on the use of the investigated quantum dots for follow-up research.

Contents

1	Introduction	7
2	Theory	9
2.1	Fluorescence of quantum dots	9
2.2	Resolution and confocal microscopy	10
3	Setup and samples	13
3.1	Experimental setup and conditions	13
3.2	Technical acquisition and data processing	16
3.2.1	Spatial scanning	16
3.2.2	Luminescence decay	17
3.2.3	Bleaching and blinking	18
3.3	Alignment procedure	19
3.4	Samples	20
3.5	Equipment	22
3.6	Notes on setup development	23
4	605 nm organic quantum dots	25
4.1	Introduction	25
4.2	Spatial scans	25
4.3	Luminescence decay	28
4.4	Bleaching and blinking	33
4.5	Conclusions	36
5	655 nm organic quantum dots	39
5.1	Introduction	39
5.2	Spatial scans	39
5.3	Luminescence decay	43
		5

5.4	Bleaching and blinking	49
5.5	Conclusions	51
6	Concluding discussion	53
7	Appendix	55
7.1	Python measurement UI	55
7.2	Python measurement classes	64

Introduction

The main aim of this research project and this thesis is to investigate the fluorescence properties of two types of commercial core-shell-structure colloidal organic quantum dots with the use of a confocal fluorescence microscope. Quantum dots are semiconductor nanocrystals that exhibit fluorescence behaviour. They can be excited by photons that surpass a specific minimum energy. They then release the absorbed energy after a certain amount of time by photons of a lower energy. A lot of research has been conducted on the behaviour of fluorescent semiconductor nanocrystals and ways to improve them. An overview of this earlier development until 2010 can be found in ref. [4]. Quantum dots offer many applications in modern technology and bio-imaging. An overview of some applications of quantum dots can be found in ref. [1] and ref. [6].

Although quantum dots are capable of fluorescence, their fluorescence behaviour and physical properties are by no means constant. Properties like particle size, absorption wavelength, emission wavelength, characteristic luminescence decay time, blinking, bleaching etc. can differ widely from one type of quantum dot to the next, or even between quantum dots of the same type. Our research addresses the spatial distribution of the quantum dots, the strength and dynamics of their fluorescence, and their luminescence decay.

A confocal fluorescence microscope was built to investigate the quantum dots. By spincoating quantum dot solutions with different concentrations on glass samples, the quantum dots could be observed in groups as well as in isolation. The details of this setup and the different samples are discussed in Chapter 3. A large portion of the experiments was automated with the use of Python scripts, which can be found in the Appendix alongside a brief explanation of the code. A description of the different mea-

surement procedures and data processing is given in Section 3.2. During the development of the experimental setup various challenges and unexpected results were encountered, and are documented briefly at the end of Chapter 3.

Chapter 4 and 5 discuss the results of the research on the two types of quantum dots in parallel. Analogous to the general order of experiments, spatial scans of the different samples are discussed and compared first. The spatial scans are succeeded by a presentation and discussion of the results concerning the luminescent decay of the quantum dots. Finally, the time-resolved dynamics of the fluorescent signal of the quantum dots are investigated.

The thesis is concluded by an overarching discussion comparing the main results of the two types of quantum dots. Finally, based on the general conclusions of this research, an advice on the further use of these quantum dots in similar or follow-up research is given.

The appendix of the thesis consists of the python code that was written to automate the different experiments coupled with a brief explanation of the UI and the different Python classes.

Theory

2.1 Fluorescence of quantum dots

Both types of quantum dots used for this research consist of a semiconductor core of CdSe (cadmium selenide) or CdTe (cadmium telluride) surrounded by a semiconductor shell of ZnS (zinc sulfide) (the manufacturer ThermoFischer Scientific does not enclose the exact composition of the quantum dots). Finally, the surface of the shell is coated with an aliphatic hydrocarbon surface, making them soluble in organic solvents. More information about the properties of the quantum dots can be found in ref. [7]

The fluorescence behaviour of a (bulk) semiconductor crystal can be described by inter-band energy transitions. The energy bands of a semiconductor are typically completely filled from the bottom up until a certain energy band, which is referred to as the 'valence band'. All energy bands above this valence band are unoccupied. The first energy band to follow the valence band is called the conduction band. The energy difference between the valence band and the conducting band is called the band-gap E_g . By the means of a photon with an energy $\hbar\omega > E_g$, an electron can be promoted from the valence band to the conducting band, leaving a hole in the valence band. The photon is absorbed in this process. The promoted electron will quickly lose its energy by emitting phonons and 'falls down' to the bottom of the conduction band. At the same time, the hole will bubble up to the top of the valence band. Therefore, the recombination of the electron-hole will typically release a photon with an energy of E_g . The result is a small emission line-width compared to the absorption spectrum. The width of this emission line typically relates to the thermal energy present among the charge carriers, with a line-width in the order of $k_B T$ at temperature T . However, the effect of rotationally and vibra-

tionally excited levels on the emission line-width can exceed the effect of the thermal energy on the line-width. In the case of nanocrystals, or quantum dots, the picture is more complex, as the electrons are confined in all spatial directions. The result of this confinement is a reduction of the energy bands into more discrete energy levels. More theory on this matter can be found in section 4.6 and appendix D.1 of ref. [3]

Quantum dots occasionally enter a temporary non-fluorescent state, also called 'blinking'. The phenomenon of blinking is reported and investigated often in other research. In 2009, Smith et al. concluded that the blinking of quantum dots can be suppressed by the use of a core/shell composition. [8] This is supported by the manufacturer, as according to them, the semiconductor shell improves the optical properties of the quantum dot. [7] Wang et al. also concluded that the nature of the core/shell composition plays a role in the prevalence of bleaching. [11] This paper was later retracted however, because the fluorescence signal they had investigated originated from defects in silica glasses. [10] Michalet et al. discuss the occurrence of blinking and several aspects of this phenomenon. [5] A statistical analysis of this blinking showed a positive correlation between the excitation intensity and the average time a quantum dot resides in a non-fluorescent state. The correlation between spectral jumps and blinking is also discussed. It was found that blinking events are often paired with drifts or jumps of the emission spectrum of a few nanometers. Finally, the influence of the environment (in particular the influence of water vapor) on the photo-physical properties is emphasized, stating that the environment can have a large influence on the emission of quantum dots and that this influence can vary between individual quantum dots.

The occurrence of bleaching is discussed rarely in other research. Van Sark et al. report bleaching after 2.5 minutes of continued exposure to a 20 kW cm^{-2} laser power. [9]

2.2 Resolution and confocal microscopy

The experimental setup that was used in this research focuses a laser beam on a sample with the use of an objective. When the laser beam is uniformly distributed over the aperture of the objective, an Airy disk is expected in the focus plane with a radius $r_0 = 0.61\lambda/\text{NA}$, relating to the spatial resolution of the setup. Therefore, the expected area A_f of the laser beam focus is $A_f = \pi r_0^2$.

As is stated in the title of the thesis, the used fluorescence microscope was built to be confocal. This means that the detected area on the sample

precisely matches the area on the sample which is illuminated by the laser, if the setup is aligned properly. This was achieved by making the part of the setup that images the laser beam onto the objective aperture and the part of the setup that captures the beam of fluorescence signal identical. The result of this confocality is that only signal is generated and received from parts of the sample that are in the focal area of the setup, eliminating out-of-focus signal. As only the focal area of the setup can be observed at a time, scanning methods must be used to image larger portions of the sample.

Setup and samples

3.1 Experimental setup and conditions

Figure 3.1 is a schematic representation of the experimental setup that was used for the experiments discussed in Chapter 4 and Chapter 5. Table 3.1 gives a description of each part of the experimental setup. The post-fiber setup was built to be confocal. The maximum power of the laser beam at the sample was measured to be ~ 1 mW and will be referred to as P_0 throughout the thesis. The background signal was minimized by blocking all sources of light as much as possible. However, the background fluorescence from the sample glass could not be suppressed and is present in all following measurements. The nature of this background signal can be observed in Figure 3.3. In addition to the background fluorescence of the sample glass, the signal of a very dim quantum dot can be seen at around $z = 68$. The background of the fluorescence glass varied from ~ 1400 counts/s to ~ 600 counts/s in this setup at a laser power of P_0 , depending on z-position of the focus and the applied laser power. In a non-confocal version of the setup, the background fluorescence signal of the glass reached intensities up to $2 \cdot 10^5$ counts/s, where the single-mode detection fiber was replaced by a multi-mode fiber with a 50 micron core. In this version of the setup, the background fluorescence of the glass was also found to exhibit a slight saturation of signal strength when increasing the laser power. All experiments were carried out at room temperature.

The emission spectrum of the 605 nm quantum dots was measured with the Ocean Optics QE65000 spectrometer and shown in figure 3.2. The spectrometer was put in place of the single photon counting module in the setup and connected to a multi-mode optic fiber with a 50 μm core instead of a single-mode fiber. On the right of the Figure the signal of the 520 nm

laser can be seen, already partially filtered out by the dichroic mirror. Next to the laser signal, a second signal peak can be observed around 540 nm. The source of this peak is unknown. Finally, a third peak around 605 nm can be observed, corresponding to the emission spectrum of the 605 nm quantum dots.

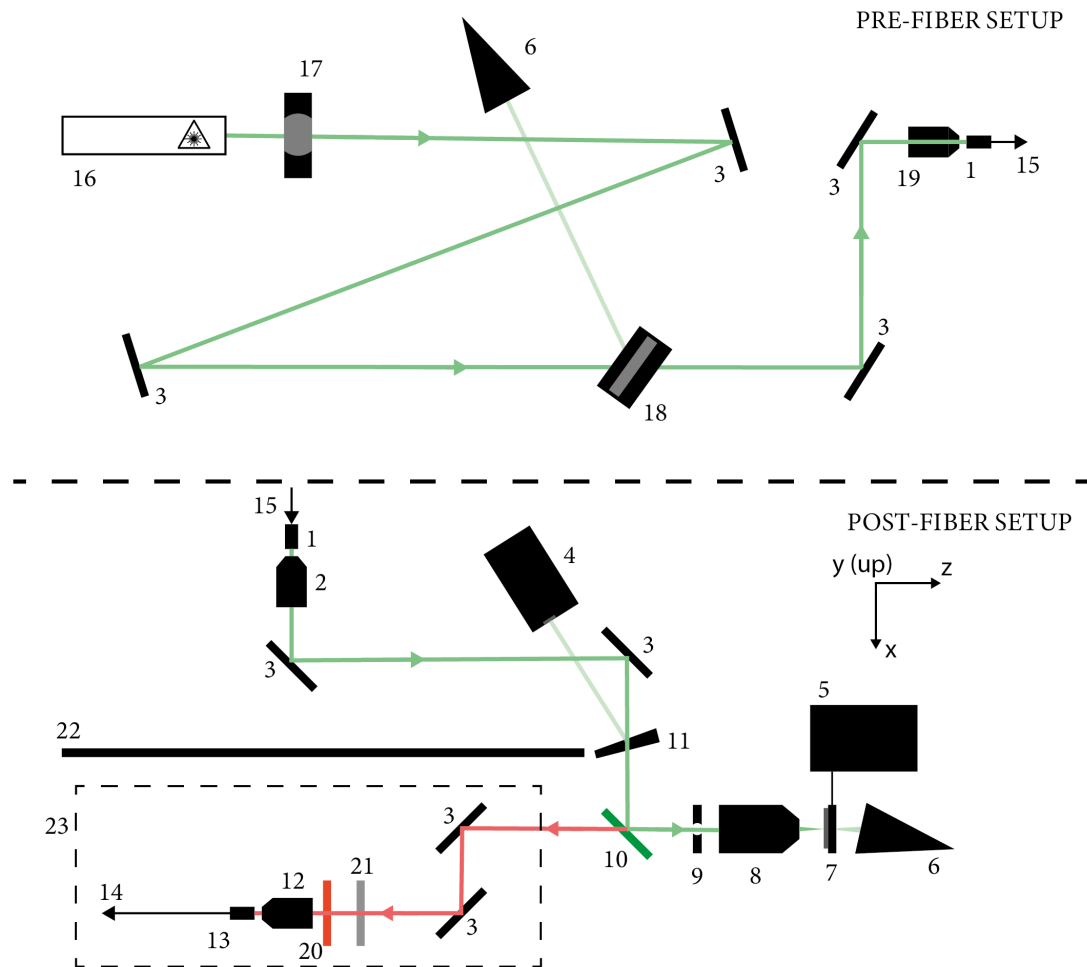


Figure 3.1: Schematic representation of the experimental setup. Distances are not to scale.

number	description
1	single mode optic fiber with a NA=0.14, transporting the laser from the upper setup to the lower setup
2	20x objective with a NA=0.17
3	Achromatic mirror
4	HUV-1100 BG Photodiode with variable resistance. Used to measure the laser power indirectly
5	PI E-517 piezo controller and piezo used to manipulate the position of the sample (7) with high precision
6	Beamdump
7	Sample
8	100x objective with a NA=0.90, mounted to a platform that can be translated in the z-direction with a μm precision
9	Aperture set to laser beam width
10	Dichroic mirror (DMLP550: 50% T/R at 550 nm)
11	Wedge prism. Redirects a small portion of the laser beam ($\sim 5\%$) into the photodiode sensor
12	20x objective with a NA=0.17
13	single mode optic fiber with a NA=0.14, transporting the fluorescence signal to the single photon counting module (SPCM)
14	single photon counting module (SPCM-AQRH-14-FC and SPCM-AQR-14-FC). For more details on the SPCM, see ref. [2]
15	connection between the pre-fiber setup and the post-fiber setup
16	ALPHALAS PICOPOWER-LD 520 nm laser, used in both continuous wave mode as pulsed mode
17	Thorlabs LCC1620 Liquid Crystal Optical Shutter, used to control the laser power focused on the sample
18	Blue filters to filter out additional wavelengths besides the 520 nm laser beam (Thorlabs FB530-10)
19	10x objective with an NA=0.17
20	Thorlabs MF630-69 (red/orange) color filter, with a transmission spectrum of 630 ± 69 nm
21	Occasional 10x or 100x achromatic filter in order to reduce the signal strength
22	Black screen blocking laser light from the upper part of the setup
23	Contraption of cardboard covering up the indicated part of the setup to prevent background light from entering the optic fiber

Table 3.1: List of used materials in experimental setup, shown in Figure 3.1.

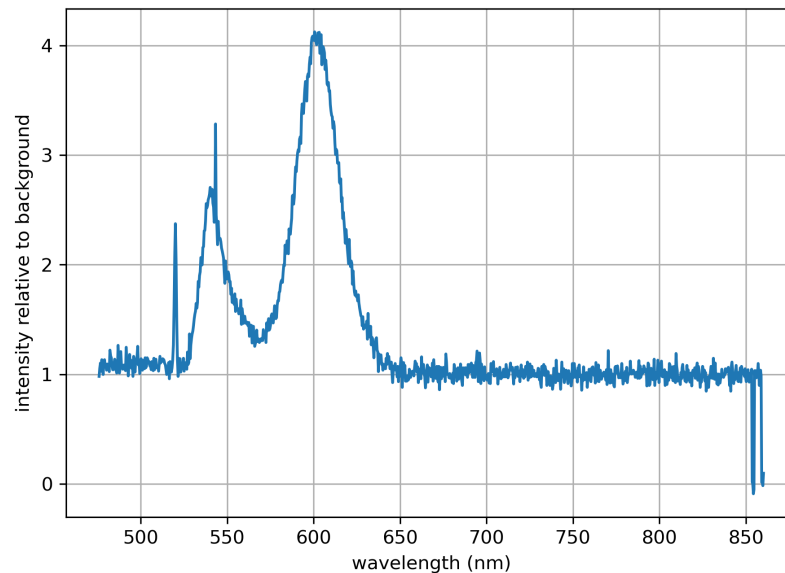


Figure 3.2: Emission spectrum of the 605 nm quantum dots relative to the background signal before signal filtering (except for the dichroic mirror).

3.2 Technical acquisition and data processing

This section reviews the different methods used in this research in detail. In addition, methods of data preparation are discussed.

3.2.1 Spatial scanning

Spatial scans involved recording the fluorescence signal strength in counts/s at different positions on the sample. After the setup was aligned and focused properly (see Section 3.3), The PI E-517 was set to an initial position of choice. Afterwards, the sample was repeatedly translated by the piezo controller in the x direction for a desired number of steps s over a length d of choice and then translated in the y direction similarly, each time a line in the x direction was completed. Therefore, in order to read the data points in chronological order, one must read the spatial scans from left to right and then from bottom to top. At each location, the fluorescence signal strength was recorded and stored in a digital, 2-dimensional array. Using a false-color scale, the data from the array was plotted in a 2-dimensional

figure. The range of the false-color scale was adjusted to the minimum and maximum fluorescence signal value of the measurement, or in some cases set to the upper and lower bound of the SPCM detection rate range.

3.2.2 Luminescence decay

The luminescence decay was measured with the use of the th260 board and the matching TimeHarp software. The sample was illuminated with laser pulses triggered by a built-in trigger generator at a frequency of 1 MHz (generated by the ALPHALAS Picosecond Pulse Diode Laser and driver). This trigger signal was also routed to the sync input of the th260. After each laser pulse was fired, the th260 recorded the detection time of the incoming fluorescence photons relative to the last received trigger signal. The detected photons were counted and distributed over $32768 = 2^{15}$ 0.025 ns bins, with a total range of $2^{15} * 0.025 \text{ ns} = 819.2 \text{ ns}$. Comparing this measurement range to the period of the pulsed laser of $1/10^6 \text{ Hz} = 1 \mu\text{s}$, we find a measurement 'duty cycle' of 82%. This 'duty cycle' will be used later on in the thesis to compare background signals.

The result of this photon event binning is a histogram showing the amount of photons that were detected after a certain amount of time after the last received trigger signal. Measurements of different duration have been carried out, typically between 180 and 3600 s. After each measurement, the data was super-binned in order to increase the signal to noise ratio. Because of a delay between the trigger signal and the fluorescence signal photons, the decay curves were preceded by $\sim 120 \text{ ns}$ of background signal. The average value of this background signal was calculated and subtracted from all data points. Data points that became negative as a consequence of this subtraction were then omitted from the data set. In order to compare different measurements more effectively and to create proper fit functions, the data points were then translated in such a way that the peak value of the luminescence decay is always found at $t = 0$.

With the `scipy.optimize` Python library and its `optimize.curve_fit` function, the resulting data was fitted with a single exponential decay template function (SEDTF) and a double exponential decay template function (DEDTF). The SEDTF is defined as follows:

$$I_{\text{single}}(t) = A \exp\left(-\frac{t}{\tau}\right). \quad (3.1)$$

The parameters A and τ signify amplitude in counts/bin and characteristic decay time in ns respectively and were optimized to the data.

The DEDTF is defined as:

$$I_{\text{double}}(t) = A \exp\left(-\frac{t}{\tau_1}\right) + B \exp\left(-\frac{t}{\tau_2}\right). \quad (3.2)$$

Again, parameters A , B and τ_1 , τ_2 signify amplitude in counts/bin and characteristic decay time in ns respectively. Both fitting functions do not include a background parameter, as the background signal has already been subtracted from all data points when the fitting procedure is executed.

Because of the exponential nature of the data, data values at the start of measurements have a higher weight in the curve optimization algorithm compared to data values that occur later in the decay curve. This bias was counteracted by fitting the square root of the equations to the square root of the data points. The resulting fit was applied to the first two decades of decay of the data only, as longer time scales are not in the scope of this research. In addition, the first two nanoseconds after the peak value of the decay are not used for the fitting process in order to exclude potential jitter around the initial peak. Using the optimized parameters of the fitted functions, the characteristic decay times of the exponential decay of the quantum dots were estimated. Finally, after the fitting procedure is finished, a small uniform filter with a window of 5 data points is applied to the original data to further decrease noise and is plotted alongside the fitted functions.

3.2.3 Bleaching and blinking

Using the Time-Tagged Time-Resolved (TTTR) mode of the th260, fluorescence photon events were recorded for a duration of 120 s and time-tagged with a temporal resolution of < 25 ps. The recorded events were then distributed over 0.1 s bins. The measurements were used to investigate the time resolved dynamics of the fluorescence signal of quantum dots.

3.3 Alignment procedure

The following procedure was carried out before measurements in order to optimize alignment and signal power of the setup.

1. The z-position of the objective is adjusted until a focus of the laser beam is seen in the detection arm behind the dichroic mirror. This focus point corresponds to either the reflection of the laser at the front of the sample glass or the back of the sample glass. The position is set in order to focus the laser beam on the front of the glass sample.
2. The red 630 nm color filter is removed temporarily and the signal received by the SPCM in counts/s is maximized by adjusting various elements of the setup. Generally, the position of the optic fiber connected to the SPCM is optimized in combination with the two preceding achromatic mirrors. Occasionally, a 10x or 100x achromatic filter is used in order to prevent saturation of the SPCM.
3. The red 630 nm color filter is placed back in position. A z-scan is carried out in order to find the z-position of the sample where the laser beam is focused on the surface of the sample glass. A typical z-scan is showed in Figure 3.3. At small z-positions, the fluorescence from the glass is visible. As the focus of the laser beam exits the glass by increasing the distance between the objective and the sample, the signal transitions to the dark count rate of the SPCM (~ 600 counts/s).
4. The z-position of the sample is set to the transition point from air to sample glass. Then a spatial scan is performed in order to find sources of fluorescence signal on the sample. If a source is found, the sample position is set to the corresponding coordinates of this source.
5. When the laser is focused on the fluorescent object, another z-scan is performed in order to find the z-position resulting in the maximum fluorescence signal.
6. Once a maximum is found, the z-position of the optic fiber connected to the SPCM is optimized to the new z-position of the sample. Then another z-scan is performed in order to find the new optimal position. This is repeated twice.

After following the previous steps, the experimental setup was aligned properly and was used for various experiments.

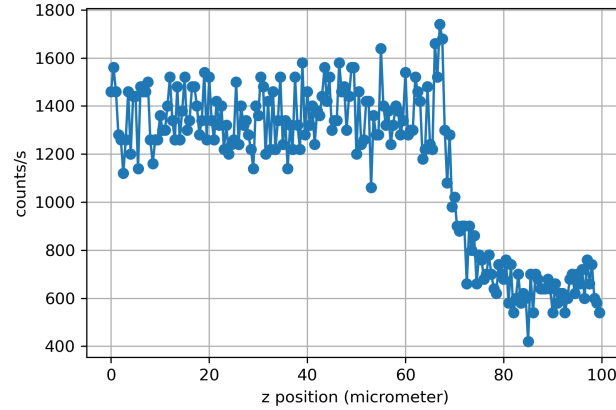


Figure 3.3: Fluorescence signal strength versus the z-position of the sample relative to some fixed point (parallel to the distance vector between the objective and the sample).

3.4 Samples

The samples that were used in this research were made using the following three solutions:

Solution 1:

50 μl PMMA in anisol 4.5% mixed with 50 μl 605 nm quantum dot solution in decane (1 μM quantum dots) and then sonicated for 5 min.

Solution 2:

6000 μl 4.5% PMMA in anisol mixed with 1 μl 605 nm quantum dot solution in decane (1 μM quantum dots) and then sonicated for 5 min. We can calculate the amount of quantum dots in a cubic micrometer solution as follows:

$$\frac{10^{-6} \text{ M/L}}{6000} = 1.7 \cdot 10^{-10} \text{ M/L} = 1.7 \cdot 10^{-25} \text{ M}/\mu\text{m}^3 \approx 0.1 \text{ particle}/\mu\text{m}^3.$$

We find that the resulting concentration is 0.1 qdots/ μm^3 .

Solution 4:

6000 μl 4.5% PMMA in anisol + 1 μl 655 nm quantum dot solution in unknown solvent (unknown Molar concentration of quantum dots) sonicated for 5 min.

Solution 5:

600 μl 4.5% PMMA in anisol + 20 μl 655 nm quantum dot solution in unknown solvent (unknown Molar concentration of quantum dots) sonicated for 5 min.

The 605 nm quantum dot solution in decane was manufactured by ThermoFischer Scientific (formerly called Life Technologies) and are 5 years old at the time of measurement. The manufacturer does not enclose details about the structure of the quantum dots. The quantum dots consist of either a CdSe or CdTe core with a semiconductor shell of ZnS. According to the manufacturer, the quantum dots have a diameter of approximately 20 nm. [7]

The 655 nm quantum dot solution was also manufactured by ThermoFischer Scientific but has an unknown age. Similar to the 605 nm quantum dots, the exact structure of the quantum dots is unknown. The solution has an unknown Molar concentration of quantum dots, solved in an unknown solvent. Although the manufacturer strongly discourages freezing, the solution was frozen in water for an unknown amount of time.

Using the former solutions, different quantum dot samples have been prepared and are listed below.

Sample 3:

Solution 1 spincoated for 1 min at 2000 rpm.

Sample 6:

Solution 2 spincoated for 1 min at 1500 rpm.

Sample 10:

Solution 4 spincoated for 80 s at 1500 rpm.

Sample 11:

Pure 655 nm quantum dot solution spincoated for 1 min at 1500 rpm.

Sample 12:

Solution 5 spincoated for 45 s at 2000 rpm.

3.5 Equipment

ALPHALAS Picosecond Pulse Laser Diode (520 nm)

The ALPHALAS Picosecond Pulse Laser Diode (520 nm) offers both a continuous wave mode and a pulsed mode with a pulse width smaller than 60 ps. The continuous wave mode was used primarily for the creation of cross section scans of the different samples and time traces, whereas the pulsed mode was used to measure the luminescence lifetime of different quantum dots and clusters. The continuous wave mode provides a peak power of ~ 15 mW collimated, coherent 520 nm light, whereas the pulsed mode provides pulses with a peak power of ~ 200 mW. A lot of power from the laser is lost by spectral filtering, transmission through a single-mode fiber and reflection from a dichroic and other mirrors before the beam reaches the sample. The laser power that finally arrives the sample is ~ 1 mW, which will be referred to with P_0 throughout the thesis. The average power of the pulsed laser mode obviously depends on the pulse frequency, which can be set by the internal trigger source of the ALPHALAS laser diode driver. Generally the maximum average pulse power was 10^{-3} of the maximum continuous wave power at a typical pulse frequency of 500-1000 kHz.

Single Photon Counter Module

A PerkinElmer single photon counter module (SPCM) was used to detect the incoming fluorescent photons from the quantum dots. It uses an avalanche photodiode to convert photons into an electrical pulse that is processed by the th260. It has a wavelength range of 400 nm to 1060 nm, which includes the typical 605 nm and 655 nm fluorescence wavelengths of the relevant quantum dots. Two versions of this type of single photon counter have been used. The SPCM-AQRH-11 has a dark count rate of ~ 2000 counts/s and will be referred to as the 'old' SPCM. The SPCM-AQRH-14 has a dark count rate of ~ 500 counts/s and will be referred to as the 'new' SPCM. Both detectors have a dead time of 32 ns and a photon detection efficiency of $\sim 60\%$ at a detection wavelength of 600 nm and a detection efficiency of $\sim 65\%$ at a detection wavelength of 650 nm.

PicoQuant TimeHarp 260 (PICO)

The TimeHarp 260 (th260) is a time-correlated single photon counting PCIe board that is able to resolve the time-difference between single photon

events detected by the SPCM with a 25 ps resolution. The time resolution of 25 ps makes this device very suitable for the investigation of fluorescent properties of matter on a microscopic scale. In this research, the TimeHarp 260 board is used for determining the photon rate of emission, for resolving the characteristic time of fluorescent decay and to make time traces in order to capture time resolved dynamics of the sources of fluorescence.

3.6 Notes on setup development

A compact list of encountered problems during the development of the setup (and their solutions) is given below.

- In order to minimize the background fluorescence signal of the sample glass, a series of orange color filters was originally placed between the dichroic mirror and the detection optic fiber. It was later discovered that the orange filter introduced unexpected artefacts, as can be seen in Figure 3.4. Afterwards, the orange filters were removed.
- Another problem that can be observed in Figure 3.4 is the recorded after-pulsing of the pulsed laser instead of the expected single pulse. This was eventually fixed by setting the Constant Fraction Discriminator (CFD) zero crossing level to -10 mV and the CFD trigger level to -30 mV. The exact reason why this solved the problem is unclear.
- Single quantum dots and small quantum dot clusters were discovered to have a relatively low fluorescence signal strength. A dark count rate of 1000 counts/s was too high for the detection of these weaker sources of fluorescence. The 'old' SPCM was replaced with another 'new' SPCM with a lower dark count rate.
- The fluorescence signal of the high density samples was high enough to saturate the SPCM. It is advised to set the laser power with caution so to not saturate and potentially damage the detection devices.
- Formerly, a multi-mode optic fiber (MMF) was used to receive the fluorescence signal photons as it made alignment of the experimental setup easier. However, replacing the MMF with a single-mode optic fiber drastically decreased the background signal.

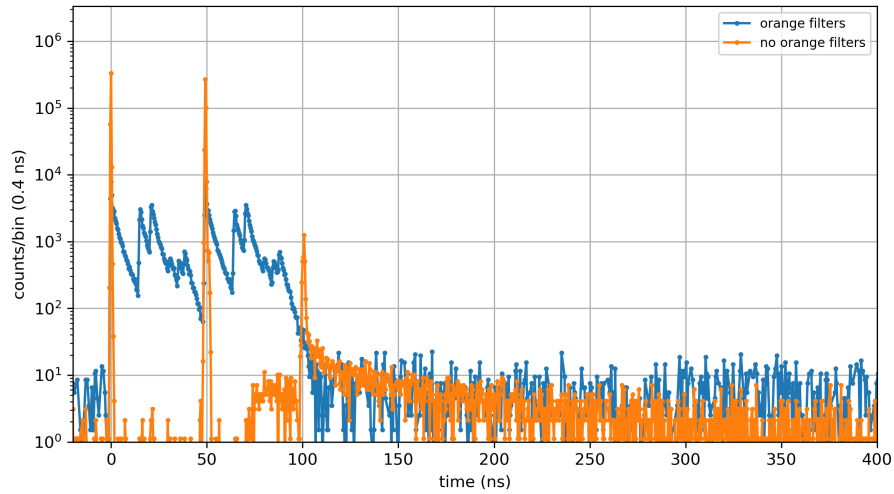


Figure 3.4: Comparison of the pulsed laser signal without orange color (orange) filters versus the pulsed laser signal with orange color filters (blue).

605 nm organic quantum dots

4.1 Introduction

This chapter describes the fluorescence properties of the colloidal 605 nm quantum dots. The properties of the fluorescence signal, fluorescent decay and bleaching and blinking behaviour have been investigated and the results are discussed and compared with theoretical models (for more details on the research methods, see Section 3.2). Two different samples were studied: *Sample 3*, created with a solution with a high concentration of quantum dots and *Sample 6*, created with a solution with a low concentration of quantum dots (more details of the samples can be found in Section 3.4). All experiments have been carried out on both samples and are then compared. Finally, the chapter ends with conclusions based on the reported experimental results.

4.2 Spatial scans

Results

A typical spatial scan of *Sample 3* with a high density of quantum dots can be seen on the left of Figure 4.1. It shows fluorescent signal varying from $2.8 \cdot 10^4$ counts/s to $3.0 \cdot 10^5$ counts/s, with a dark count rate of ~ 600 counts/s. The local maxima have an average FWHM of $\sim 1.6 \mu\text{m}$. This scan was carried out with a laser power of $10^{-2}P_0$ in order to prevent bleaching and saturation of the SPCM.

On the right of Figure 4.1, a typical spatial scan of *Sample 6* with a low density of quantum dots is shown. The fluorescent signal varies between

$5 \cdot 10^2$ and $3 \cdot 10^3$ counts/s, with the same dark count rate. The background fluorescence signal of ~ 1000 counts/s of the sample glass can also be observed (see Section 3.3 for more details about the glass fluorescence). Similar to the high density sample, the local maxima of the low density sample have a FWHM of $\sim 1.6 \mu\text{m}$. The corresponding scan was carried out with a laser power of $0.2P_0$ in order to prevent bleaching.

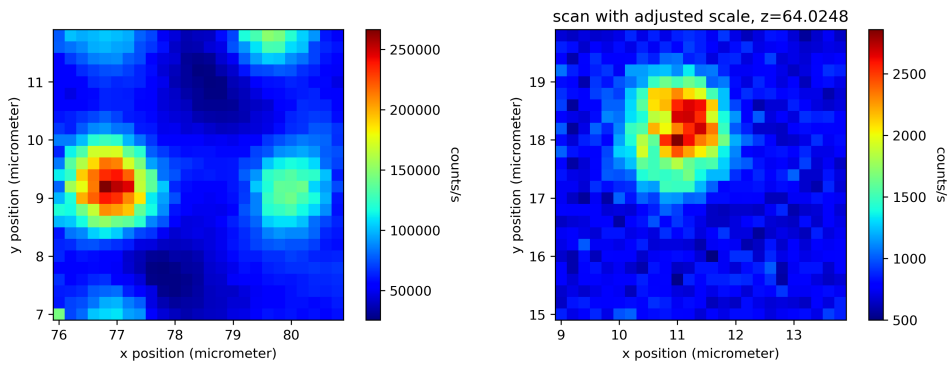


Figure 4.1: Spatially resolved fluorescence of high and low density samples. Left: High density sample (Sample 3) measured with a laser power of $0.01P_0$. Right: Low density sample (Sample 6) measured with a laser power of $0.2P_0$. The scale of both images is adjusted to the upper and lower bounds of the corresponding data.

Discussion

Comparing the spatial scan of *Sample 3* with *Sample 6* in Figure 4.1, pronounced differences between the intensities of the local maxima of fluorescent signal can be observed. Accounting for the difference in laser power that was used during scanning and the fluorescence signal from the sample glass, we see a $(0.2/0.01) \cdot (3 \cdot 10^5 / 2 \cdot 10^3) = 3000$ fold increase in signal strength. Both scans show a similar spatial resolution, with a FWHM of $\sim 0.8 \mu\text{m}$ for local maxima. The theoretical limit of the spatial resolution of this setup using a microscope objective with a NA of 0.9 was determined to be $0.35 \mu\text{m}$ (see Section 2.2). Comparing this to the scanning results, we find an actual spatial resolution about 2 times the theoretical limit. This is expected, as the microscope objective was under-filled in order to maximize laser power on the sample. As the FWHM is independent on the fluorescent signal strength, it follows that

$$d_{\text{object}} \ll r.$$

where d_{object} is the radius of the imaged fluorescent objects and r the spatial resolution. This is in agreement with the size estimation of the manufacturer, stating that the overall size of the quantum dots is approximately 20 nm. [7] The independence of the width of the local maxima on their maximum fluorescence signal shows the quantum dots have a high tendency to cluster together.

This observation yields that the amount of quantum dots located in a cluster is proportional to its fluorescence signal, meaning that the high density sample quantum dot cluster on the left of Figure 4.1 contains an order of 3000 times more quantum dots compared to the cluster shown on the right.

4.3 Luminescence decay

Results

Figure 4.2 shows the luminescence lifetime of the big cluster, earlier introduced on the left of Figure 4.1. The measurement was carried out with a pulsed laser signal with an average laser power of $10^{-3}P_0$ and pulses with a width less than 60 ns and a pulse peak power of 200-250 mW. A background level of 492.2 counts/bin was subtracted from the original data set. With a total of 1024 0.8 ns bins and a measurement duration of 180 s, we can calculate the background signal in counts/s:

$$\frac{492.2 \text{ counts/bin}}{180 \text{ s} \cdot 0.82} \cdot 1024 \text{ bins} = 3.41 \cdot 10^3 \text{ counts/s.}$$

Where the value of 0.82 is the measurement duty cycle (for more information of the measurement duty cycle, see Section 3.2). This background signal is in agreement with the earlier measured background count rate levels of the old SPCM (see Section 3.5). Data points that ended up below zero after background subtraction have been omitted from the data (for more details on the data preparation and analysis process, see Section 3.2). We compare the shape of the luminescence decay of the quantum dot cluster with the optimized SEDTF (see Section 3.2). The resulting fit is shown in green in Figure 4.2, with optimized parameters $A = 1.3 \cdot 10^5$ counts/bin and $\tau = 20.2 \pm 0.1$ ns.

In addition to the SEDTF, the data is also compared to the optimized DEDTF. The resulting fit is shown in red in Figure 4.2, with optimized parameters $A = 8.1 \cdot 10^4 \pm 0.2 \cdot 10^4$ counts/bin, $\tau_1 = 14.0 \pm 0.2$ ns, $B = 5.4 \cdot 10^4 \pm 0.2 \cdot 10^4$ counts/bin and $\tau_2 = 26.4 \pm 0.3$ ns.

Figure 4.3 shows the time-resolved fluorescence on various spots around the same local maximum of fluorescence signal on *Sample 6*. Again, the measurements were carried out with a pulsed laser signal with an average laser power of $10^{-3}P_0$ and pulses with a width < 60 ns and a peak power of 200-250 mW. A noise level of 325.4 counts/bin was subtracted from the data. Using the SEDTF and parameter optimization, we find the optimized parameters $A = 5.2 \cdot 10^2 \pm 0.3 \cdot 10^2$ counts/bin and $\tau = 7.5 \pm 0.4$ ns for the sum of all measurements, illustrated in purple in Figure 4.3. The fits of this sum of the measurements are shown in Figure 4.4. We find that the characteristic decay time τ for the individual measurements is within a 1 ns range of the collective characteristic decay time of 7.5 ns, which can also be observed in the figure. In contrast, the fluorescence signal strength was found to vary with the spatial scanning location.

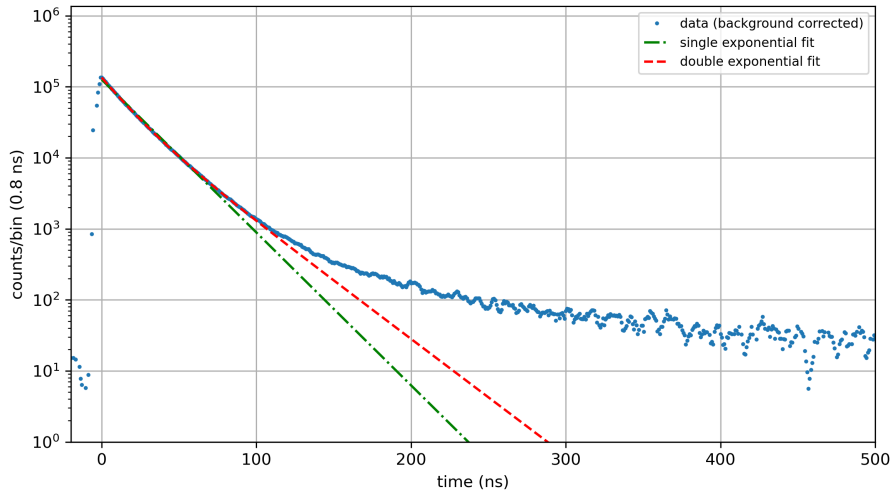


Figure 4.2: Decay trace of a bright quantum dot cluster compared to two exponential fitting functions. Green: single exponential fit function (see Equation 3.1). Red: double exponential fit function (see Equation 3.2).

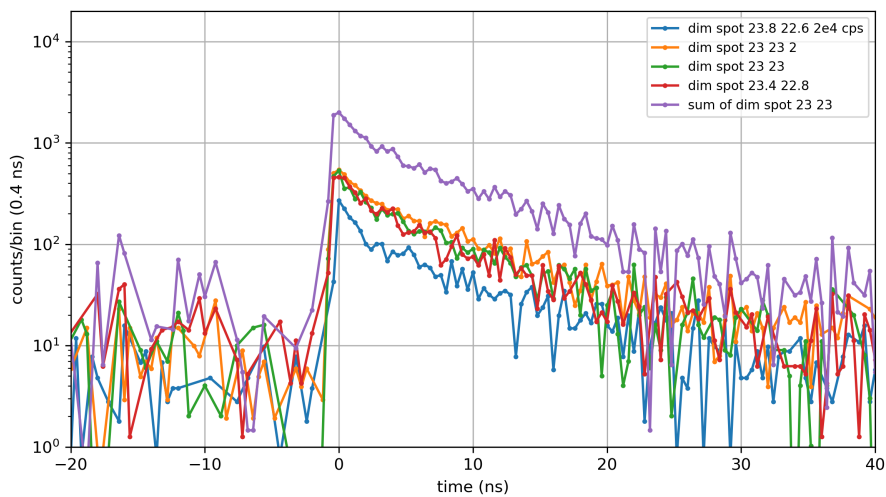


Figure 4.3: Luminescence decay of a dim quantum dot cluster measured on different locations.

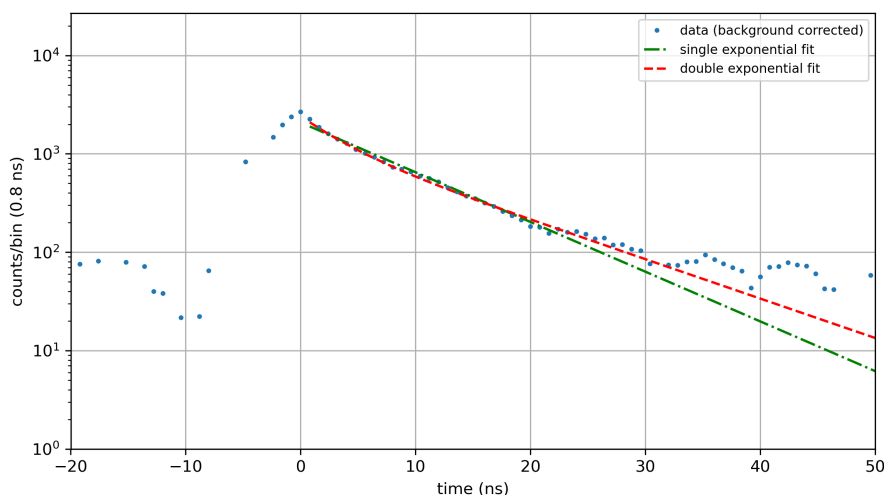


Figure 4.4: Luminescence decay of the sum of the measurement shown in Figure 4.3. The single exponent fit decay rate was found to be 8.6 ± 0.3 ns. The double exponent fit decay rates were found to be 3.3 ± 1.5 ns with a relative magnitude of 0.4 and 11 ± 1.7 ns with a relative magnitude of 0.6.

Figure 4.5 shows the luminescence decay of different sources of fluorescence. No alterations were made to the earlier explained measurement conditions for the measurements of Figure 4.5. The blue line represents a bright cluster on the low density sample that was measured for 360 s, the yellow line shows a summation of two 1800 s measurements on a dim cluster on the low density sample and the purple line illustrates the luminescence decay of a very dim cluster measured over a period of 900 s, also measured on the low density sample. In addition, the earlier introduced luminescence decay from Figure 4.2 is shown in green in Figure 4.5. In contrast to other figures, a bin size of 0.4 ns was chosen instead of 0.8 ns in order to preserve details of the other measurements with a lower signal strength. The sum of the measurements of Figure 4.3 is also shown in red in Figure 4.5. Because the duration of the different experiments differ, the signal strength can not be compared based on this figure. Using the SEDTF, we find the characteristic decay times τ for the measurements that are included in the corresponding figure shown in Table 4.1.

Figure 4.6 compares the luminescence decay of three different 605 nm quantum dot clusters. The blue line in this figure represents a 1800 s measurement of a very dim quantum dot cluster, also shown in Figure 4.8.

Line color	τ	measurement time
Green (<i>Sample 3</i>)	20.2 ± 0.1 ns	180 s
Red (<i>Sample 6</i>)	7.5 ± 0.4 ns	720 s
Yellow (<i>Sample 6</i>)	4.4 ± 0.3 ns	3600 s
Blue (<i>Sample 6</i>)	7.7 ± 0.4 ns	360 s
Purple (<i>Sample 6</i>)	6.1 ± 1.2 ns	900 s

Table 4.1: list of characteristic decay times τ corresponding to Figure 4.5.

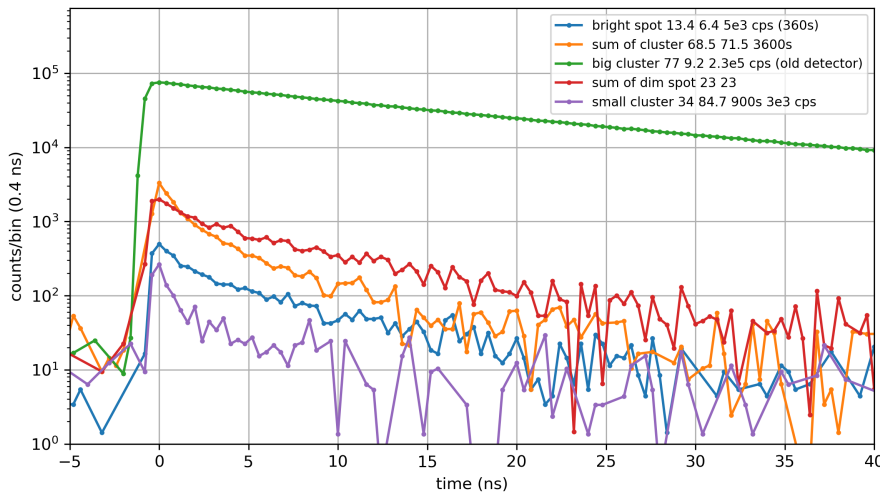


Figure 4.5: Comparison of fluorescent decay curves. Corresponding characteristic decay times can be found in Table 4.1. Because experiments differ widely in duration, the signal strength can not be compared in a meaningful way.

Discussion

The luminescence decay of a quantum dot cluster was fitted using equations 3.1 and 3.2 (see Section 3.2), shown in Figure 4.2. We find that during the first decade of decay, the luminescence decay of the quantum dot cluster can be described by the SEDTF, with optimized parameters $A = 1.3 \cdot 10^5$ counts/bin and $\tau = 20.2 \pm 0.1$ ns. After the first decade, the luminescence decay can no longer be accurately described by the SEDTF. Comparing the luminescence decay with the optimized DEDTF, we find that the luminescence decay can be accurately described with this function, using optimized parameters $A = 8.1 \cdot 10^4 \pm 0.2 \cdot 10^4$ counts/bin, $\tau_1 = 14.0 \pm 0.2$ ns, $B = 5.4 \cdot 10^4 \pm 0.2 \cdot 10^4$ counts/bin and $\tau_2 = 26.4 \pm 0.3$ ns.

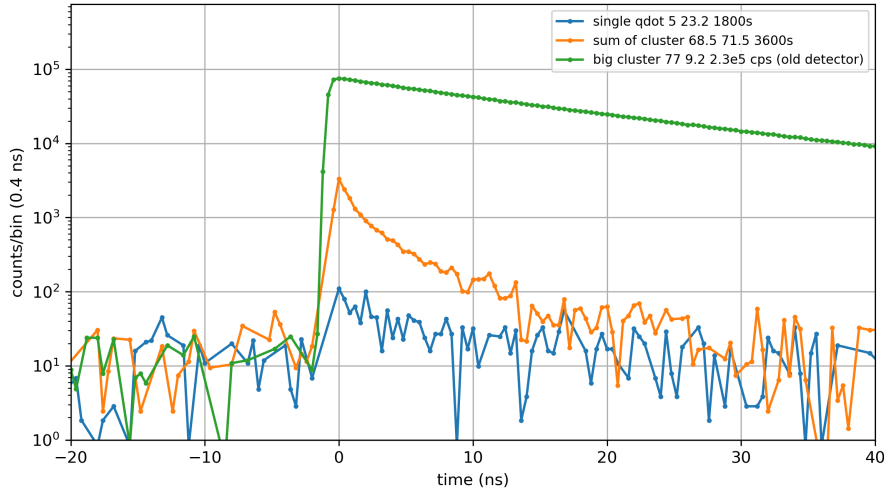


Figure 4.6: Comparison of measurements on three different 605 nm quantum dot clusters. Green: Very bright quantum dot cluster. Yellow: Dim quantum dot cluster. Blue: Very dim quantum dot cluster (possibly a single quantum dot).

After two decades of decay, the DEDTF also fails to describe the measurements accurately. Domains beyond the second decade of decay are however not in the scope of this research. If we analyse the optimized parameters of the DEDTF, we find that the faster decay component accounts for $8.1 \cdot 10^4 / (5.4 \cdot 10^4 + 8.1 \cdot 10^4) \approx 0.6$ part of the decay and the slower decay component for 0.4.

We conclude that the initial nanoseconds of luminescence decay of the 605 nm quantum dots can be described by the SEDTF.

Analyzing the results from Figure 4.3, we find that the found characteristic decay time τ is likely independent from spatial variations in contrast to signal strength. This reinforces the assumption that $d_{\text{object}} \ll r$.

Comparing the results from Figure 4.2 and Figure 4.3, we find large differences in apparent characteristic decay time τ . This variety in characteristic decay times is illustrated further in Figure 4.5 and Table 4.1 and show characteristic decay times ranging between 4.4 ns and 20.2 ns. In general, we found that brighter quantum dot clusters have longer characteristic decay times than quantum dot clusters that are more dim.

From Figure 4.6 we conclude that very dim quantum dot clusters and single quantum dots have insufficient fluorescence signal strength for a measurement of the luminescence decay.

4.4 Bleaching and blinking

Results

Figure 4.7 shows the decrease in fluorescence intensity of the quantum dot cluster shown on the right of Figure 4.1 over time when exposed to a continuous 520 nm laser signal with power P_0 . The Figure consists of 4 concatenated consecutive 120 s measurements of time tagged photon events. After each measurement, the photon events were binned in 0.1 s bins and counted. Each measurement starts with ~ 8 s of background signal with the laser turned off, resulting in the repeating plateaus separating each 120 s measurement. The plateaus have an average value of ~ 60 counts/bin, corresponding to 600 counts/s, which agrees with the dark count rate of the 'new' SPCM. The first 120 s measurement also includes a second plateau, where the laser is turned on, but focused on an empty spot of the sample, measuring the fluorescence from the sample glass. The average value of this plateau is 100 counts/bin, corresponding to 1000 counts/s, which agrees with the background signal that can be seen on the right of Figure 4.1. Over the 4 consecutive 120 s measurements the fluorescence signal strength has decreased with ~ 8500 counts/s.

In addition to the decay of fluorescence intensity over time, the quantum dot cluster showed dynamics on both the 100 ms scale as well as the seconds scale. Large fluctuations with an amplitude in the order of 10^2 counts/bin have been observed on time scales between 1 and 10 s.

Figure 4.8 shows a 120 s time trace of a different quantum dot cluster at a laser power of P_0 , similar to Figure 4.7. Again, fluctuations in fluorescence intensity were observed, but in contrast to Figure 4.7, the fluorescence signal drops to the level of background fluorescence at ~ 1200 counts/s and back to the original signal strength repeatedly. These periods of 'darkness' have a duration on time scales of 100 ms as well as seconds.

Similar to Figure 4.7, three additional measurements on the same quantum dot cluster have been carried out and are concatenated to the original measurement, resulting in Figure 4.9. Again, each measurement starts with ~ 5 s of background signal. In addition to the on-off blinking events, a decrease of ~ 1000 counts/s of the maximum fluorescence signal over the four consecutive measurements was observed. The decrease was observed to occur in steps of ~ 250 counts/s between measurements and no decrease was found during the measurements.

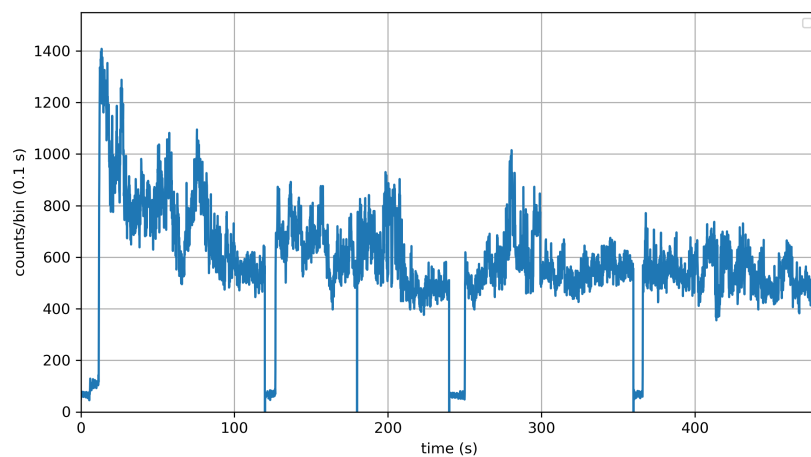


Figure 4.7: Concatenation of the four 120s time trace measurements of the quantum dot cluster on the right of Figure 4.1. Each plateau signifies the start of a new 120s measurement. The second plateau of the first measurement ($5s < t < 12s$) is the fluorescence of the sample glass, measured at a coordinate without quantum dots.

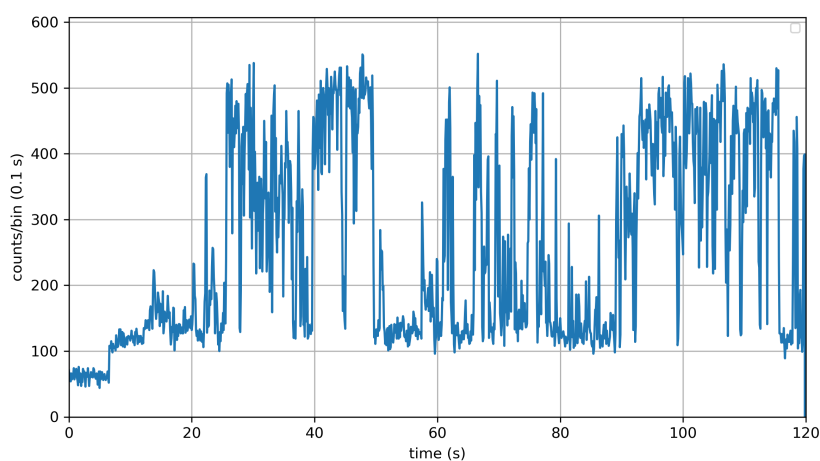


Figure 4.8: Time resolved dynamics of a very dim quantum dot cluster (first 120 seconds). Similar to Figure 4.7, the first plateau is the background signal and the second plateau is the background fluorescence signal generated by the sample glass.

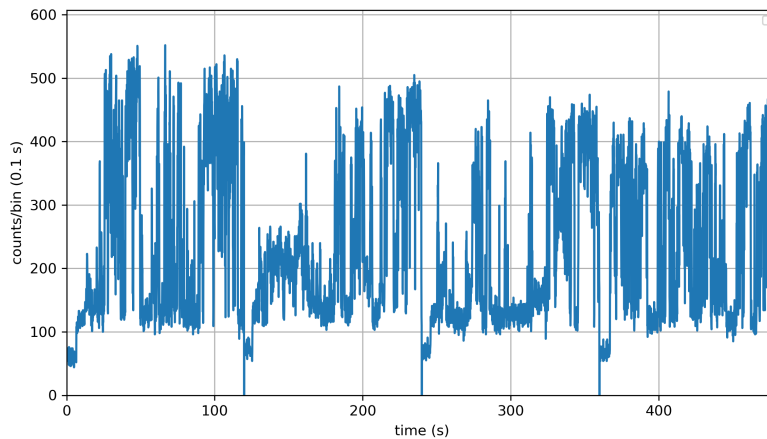


Figure 4.9: Concatenation of the four 120 s measurements of the time trace of the quantum dot cluster from Figure 4.8, measured with laser power P_0 . Each plateau signifies the start of a new 120 s measurement.

Discussion

From the time trace experiments we conclude that the 605 nm quantum dots show both blinking and bleaching behaviour, which should be taken into account during other measurements. Figure 4.7 illustrates the effect of bleaching and shows a continuous decrease of fluorescence signal. Because the decrease is gradual and continuous, we conclude that the amount of quantum dots in this cluster is high.

Figure 4.8 shows the effect of blinking. Fluorescence signal jumps of 400 counts/bin have been observed on time scales of 100 ms as well as seconds to tens of seconds. Comparing Figure 4.8 to Figure 4.7 we conclude that the number of quantum dots in this cluster must be much smaller than the number of quantum dots in the cluster of Figure 4.7. The rapid and sudden jumps suggest the fluorescence signal is generated by a single quantum dot.

Conversely, the concatenation of the additional 120 s measurements of Figure 4.8, shown in Figure 4.9, shows a gradual decrease in the maximum fluorescence intensity between measurements, starting at ~ 500 counts/bin and ending at ~ 400 counts/bin. The decrease appears to happen between measurements with steps of 25 counts/bin. In addition, smaller jumps of 100 counts/bin have been observed, which can be seen around $t = 150$ s. It could be argued that the gradual decrease of fluorescence intensity was caused by a drift in the experimental setup. However, this hypothetical

drift would have induced variations in the background fluorescence signal as well, which was never observed in this or any other experiment. In addition, the hypothetical drift would also have a chance to increase the observed fluorescence signal if the setup was not aligned perfectly. This was also never observed in any experiment. We therefore conclude that the results shown in Figure 4.9 are not likely to be caused by a drift in the experimental setup. Instead, the gradual decrease and the small jumps of the fluorescence signal suggest additional contributions from other quantum dots.

4.5 Conclusions

Experiments show that the investigated 605 nm quantum dots have widely differing fluorescence characteristics. In the cross sectional scans we have observed fluorescent sources with differing signal strength up to a factor 1000-5000 and comparable FWHM sizes of $\sim 1.6 \mu\text{m}$. We conclude that the quantum dots have a high tendency of clustering. Both samples with a high concentration of quantum dots and samples with a low concentration of quantum dots show quantum dot clusters. In addition, we conclude that these quantum dot clusters have a size much smaller than the spatial resolution of the experimental setup.

The estimated characteristic decay time of the 605 nm quantum dots differs widely and ranges between 4.4 ns and 20.2 ns. The luminescence decay is only exponential in the first decade of decay and slows down on longer time scales, suggesting other, slower energy transitions play a non-negligible role in the decay behaviour of the 605 nm quantum dots. Using a double exponential decay function, the decay behaviour of the quantum dots can be described better if the signal strength was sufficient. In general, brighter clusters showed larger characteristic decay times in comparison to more dim quantum dot clusters. As the characteristic decay time was not effected by small spatial variations of the scanning coordinates, we conclude again that the size of the quantum dot clusters is much smaller than the spatial resolution of the experimental setup.

Measurements of the time resolved dynamics of collections of quantum dots show that the effects of bleaching and blinking are prevalent and should be taken into account when conducting research. Figure 4.9 shows both extreme blinking behaviour, as well as gradual bleaching effects, suggesting the fluorescence signal was generated by a single quantum dot, or that the system consist of multiple quantum dots that are in a 'dark', non-excitable state most of the time. We conclude that this blinking behaviour

hinders the detection of single quantum dots greatly in this setup and we therefore do not recommend the use of these 605 nm quantum dots in comparable or successive research projects.

655 nm organic quantum dots

5.1 Introduction

Parallel to the previous chapter, this chapter describes the fluorescence properties of the colloidal 655 nm quantum dots. The properties of the fluorescence signal, fluorescent decay and bleaching and blinking behaviour have been investigated using the same methods and the results are discussed and compared with theoretical models. Three different samples were studied: *Sample 11*, created with a solution with a (relatively) high concentration of quantum dots in comparison to the other samples, *Sample 10*, created with a solution with a (relatively) low concentration of quantum dots and *Sample 12*, created with a solution with a concentration of quantum dots between the former two samples (more details of the samples can be found in Section 3.4). Most experiments have been carried out on *Sample 10* and *Sample 11* and are then compared. Finally, the chapter ends with conclusions based on the reported experimental results.

5.2 Spatial scans

Results

A spatial scan of *Sample 11* with a high density of quantum dots can be seen on the left of Figure 5.1. It shows fluorescent signal varying from $3 \cdot 10^2$ counts/s to $5.6 \cdot 10^4$ counts/s, with a dark count rate of ~ 600 counts/s (see Section 3.2 for a description of the scanning method). The local maxima have an average FWHM of $\sim 2 \mu\text{m}$. This scan was carried out with a laser power of $10^{-2}P_0$ in order to prevent bleaching and saturation of the

SPCM. In addition to the two bright fluorescence sources, many weaker sources can be observed with counts rates of $1 \cdot 10^4$ - $2 \cdot 10^4$, surrounding the bright fluorescence sources. The middle of the image shows regions where the fluorescence signal does not surpass the background fluorescence signal of the sample glass.

The right hand part of Figure 5.1 shows a spatial scan of *Sample 10* with a low density of quantum dots. A single fluorescence source is visible at the coordinates [28, 25]. The fluorescence signal varies between $5 \cdot 10^2$ and $1 \cdot 10^3$ counts/s, with the same dark count rate. The background fluorescence signal of ~ 800 counts/s of the sample glass can also be observed (see Section 3.1 for more details about the glass fluorescence). Although the local maximum is barely distinguishable from the background signal, we verified that the maximum at the coordinates [28, 25] corresponds to a single quantum dot. This observation will be discussed later in Section 5.4. The FWHM of this maximum could not be determined from the spatial scan, as half of its value $1 \cdot 10^3/2 \approx 5 \cdot 10^2$ does not surpass the background signal. The corresponding scan was carried out with a laser power of P_0 in order to maximize the fluorescence signal strength.

Additional scans of the low density sample with a higher resolution are shown in Figure 5.2. The minimum count rate of the left scan is $7 \cdot 10^2$ counts/s and the maximum count rate is $2 \cdot 10^3$ counts/s, with the same dark count rate. From this scan, the FWHM can be determined and is estimated to be 5 - 6 pixels, or $\sim 1.2 \mu\text{m}$. An additional observation is the elongation of the x-dimension of the fluorescence source. This elongation can also be observed in the left scan of Figure 5.2.

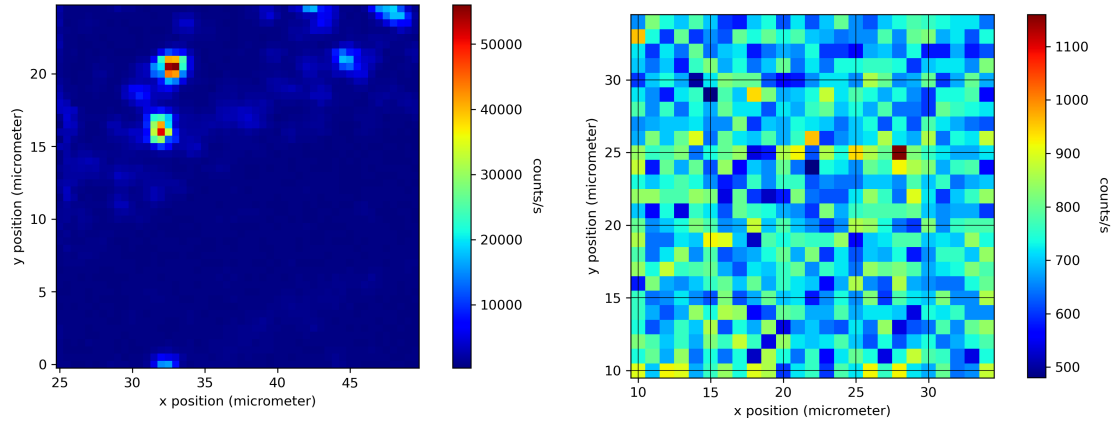


Figure 5.1: Spatially resolved fluorescence of high and low density samples. Left: High density sample (Sample 11) measured with a laser power $0.01P_0$. Right: Low density sample (Sample 10) measured with a laser power of P_0 . The scale of both images is adjusted to the upper and lower bounds of the corresponding data.

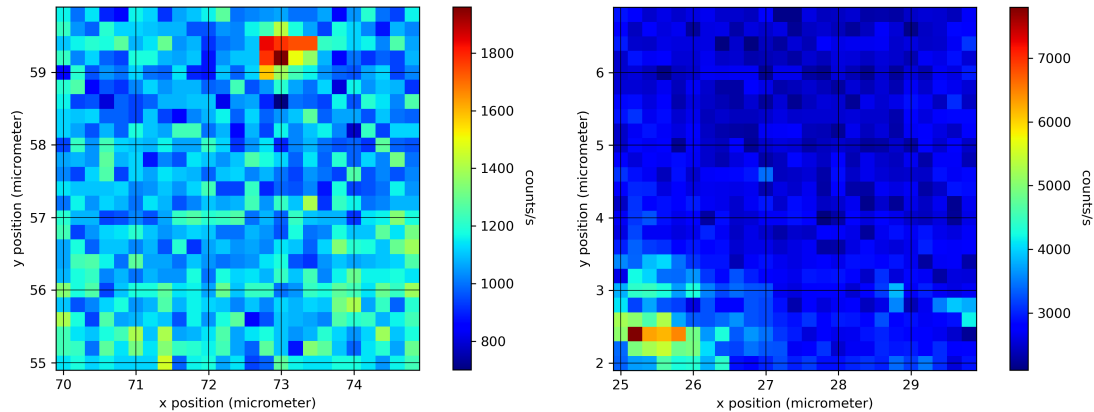


Figure 5.2: Spatially resolved fluorescence scans of two different quantum dot clusters on the low density sample with laser power P_0 . The scale is adjusted to the upper and lower bounds of the corresponding data.

Discussion

We compare the spatial scan of *Sample 11* with *Sample 10* in Figure 5.1 and find great differences between the intensities and abundances of the local maxima of fluorescent signal. Accounting for the difference in laser power that was used during scanning and the background fluorescence signal from the sample glass, we see a $(1/0.01) \cdot (5.6 \cdot 10^4 / (1 \cdot 10^3 - 700)) \approx 2 \cdot$

10^4 fold increase in signal strength when comparing the local maxima of Figure 5.1.

Both scans show a similar spatial resolution, with a FWHM of 1.2 - 2 μm for local maxima. We compare the earlier discussed theoretical spatial resolution with the scanning results and find an actual spatial resolution about 2 times the theoretical limit. We conclude that the actual spatial resolution has not changed between scans of the 605 nm quantum dots samples and the 655 nm quantum dots samples.

In addition, we reconfirm the earlier stated relation

$$d_{\text{object}} \ll r,$$

where d_{object} is the 'characteristic' length of the imaged fluorescent objects and r the spatial resolution, again conform the size approximation of the manufacturer of 20 nm. [7] The width of the local maxima shows no relation to the maximum fluorescence signal of the local maxima. We conclude that the 655 nm quantum dots have a high tendency to cluster, similar to the 605 nm quantum dots. In contrast, the left side of Figure 5.1 shows regions where only the signal strength of background fluorescence was measured, suggesting the solution of quantum dots used for spin coating was not homogeneous, resulting in super-cluster structures on the sample.

Again, if we assume the fluorescence signal that is generated by a quantum dot cluster is proportional to the number of quantum dots in the given cluster, we find that the high density sample quantum dot cluster on the right of Figure 5.1 contains an order of $2 \cdot 10^4$ times more quantum dots compared to the cluster shown on the right.

The shape of the imaged fluorescence sources in Figure 5.2 is longer along the x-axis. We attribute this variation in shape to the combination of blinking and the scanning method, where the sample is scanned from left to right and then from bottom to top. Coordinates that are adjacent in the x-direction are measured consecutively, whereas coordinates that are adjacent in the y-direction are measured after a scan in the x-direction is completed. As the time scale of dark states of quantum dots was observed to be in the order of seconds, similar to the time it took to scan a line in the x-direction, it means that the transition from a luminous state to a dark state and back of a quantum dot (cluster) is most prominently visible in the x-direction. It could be argued that quantum dot clusters cannot exhibit blinking behaviour. However, the earlier discussed Figure 4.9 shows clear blinking behaviour in the case of a fluorescence source with a fluorescence intensity of 5000 counts/s. Although the elongation in the x-direction could be caused by a misalignment in the setup, this effect was

never observed for more luminous fluorescence sources. We therefore conclude that this effect is unlikely to be caused by a flaw in the experimental setup.

5.3 Luminescence decay

Results

Figure 5.3 shows the luminescence lifetime of a bright 655 nm quantum dot cluster. The measurement was carried out with a pulsed laser signal with an average laser power of $\sim 10^{-3}P_0$ and pulses with a width of less than 60 ns and a pulse peak power of 200-250 mW. A background level of 235.5 counts/bin was subtracted from the original data set (more information on how this background level was determined can be found in Section 3.2). With a total of 1024 0.8 ns bins and a measurement duration of 540 s, we can calculate the background signal in counts/s:

$$\frac{235.5 \text{ counts/bin}}{180 \text{ s} \cdot 0.82} \cdot 1024 \text{ bins} = 5 \cdot 10^2 \text{ counts/s.}$$

Where the value of 0.82 is the measurement duty cycle (for more information about the measurement duty cycle, see Section 3.2). The value of $5 \cdot 10^2$ counts/s corresponds to the dark count rate of the new SPCM (see Section 3.5). Data points that ended up below zero after background subtraction have been omitted from the data (for more details on the data preparation and analysis process, see Section 3.2). Again, we compare the shape of the luminescence decay of the quantum dot cluster to the SEDTF. The resulting fit is shown in green in Figure 5.3, with optimized parameters $A = 1.4 \cdot 10^5 \pm 0.02 \cdot 10^5$ counts/bin and $\tau = 31.9 \pm 0.4$ ns.

In addition to the fitted SEDTF, the optimized DEDTF was also compared to the actual data. The fitted DEDTF function is shown in red line in Figure 4.2, with optimized parameters $A = 1.1 \cdot 10^5 \pm 0.01 \cdot 10^5$ counts/bin, $\tau_1 = 14.5 \pm 0.2$ ns, $B = 6 \cdot 10^4 \pm 0.1 \cdot 10^4$ counts/bin and $\tau_2 = 44.3 \pm 0.3$ ns. Figure 5.4 shows the first two decades of decay in more detail. Note the good quality of the data and the clear deviation between the data and the fitted SEDTF.

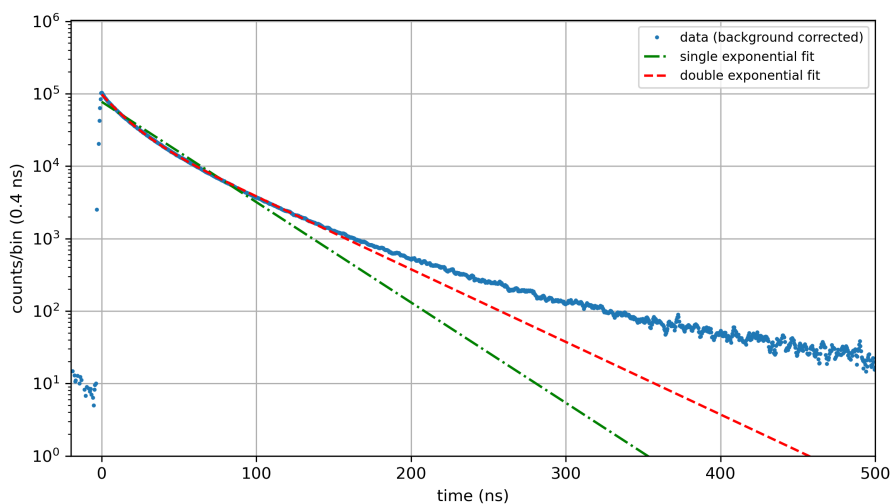


Figure 5.3: Decay trace of a bright 655 nm quantum dot cluster. The single exponent fit decay rate was found to be 31.9 ± 0.4 ns. The double exponent fit decay rates were found to be 14.5 ± 0.2 ns with a relative magnitude of 0.6 and 44.3 ± 0.3 ns with a relative magnitude of 0.4.

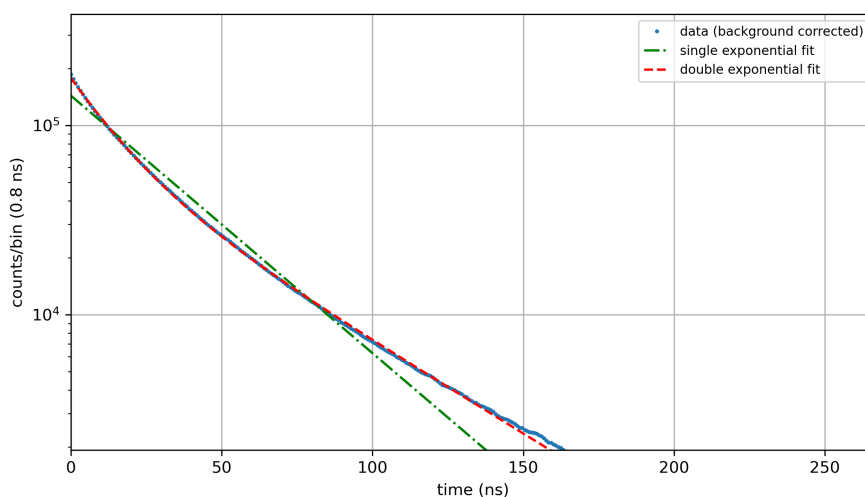


Figure 5.4: Zoomed view of the first two decades of decay of the luminescence decay first introduced in Figure 5.3.

The measurement shown in Figure 5.3 was repeated with the power of the pulsed laser reduced by a factor 1000 and is shown in Figure 5.5 alongside the measurement from Figure 5.3. The same measurements conditions apply. Using the same fitting methods, we find the following optimized parameters for the low laser power measurement: $A = 414 \pm 11$ counts/bin and $\tau = 26.9 \pm 0.7$ ns. We found a small difference in the characteristic decay time between the low and high laser power measurement. However, when we restrict the fitting procedure of the SEDTF to the first decade of decay, we found $\tau = 26.0 \pm 0.3$ ns for the high laser power measurement and $\tau = 26.3 \pm 0.7$ ns for the low laser power measurement.

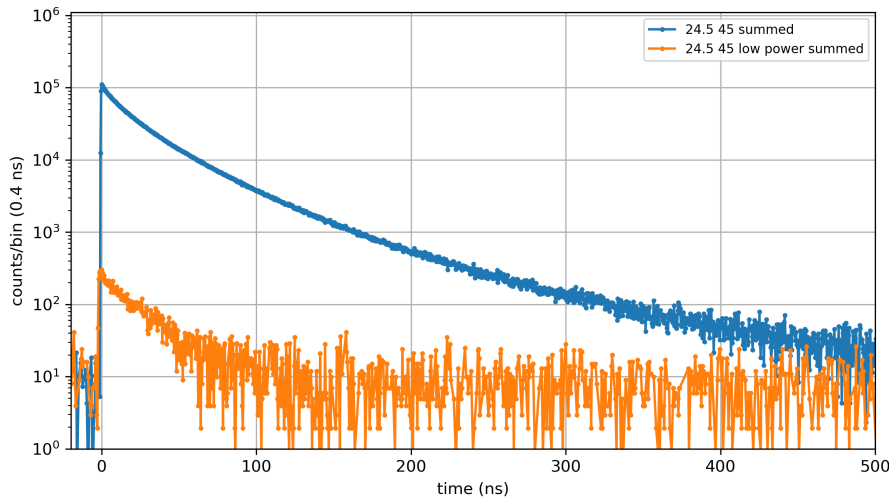


Figure 5.5: Comparison of the decay rate at low pulsed laser power ($\sim 10^{-6} P_0$) and maximum pulsed laser power ($\sim 10^{-3} P_0$).

Figure 5.7 and Figure 5.8 show further investigation of the correlation between the intensity of a quantum dot cluster and its characteristic decay time. Multiple measurements of the luminescence decay have been performed on different locations of the sample. All decay traces have been analysed using the SEDTF fit and were applied to the first decade of decay. The position-dependent count rates are indicated in the legend of Figure 5.7 and ranged from 600 counts/s to $2 \cdot 10^5$ counts/s. The position-dependent count rates were extracted from spatial scans of the high density sample (*Sample 11*), carried out with a laser power of $10^{-2} P_0$ (the count rates are position dependent because the quantum dot density differs with the spatial location). In this case, the background signal was

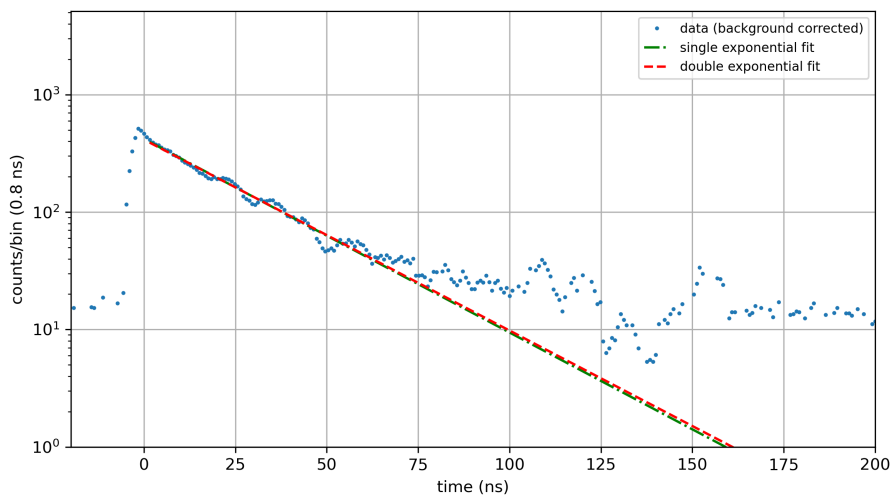


Figure 5.6: Decay trace of a bright 655 nm quantum dot cluster measured at a very low laser power and fitted using only the first decade of decay. The single exponent fit characteristic decay time was found to be 26.3 ± 0.7 ns. The double exponent fit characteristic decay times were found to be 0.01 ns with a relative magnitude of 0.1 and 26.7 ± 0.8 ns with a relative magnitude of 0.9.

not subtracted, as the spatial scan from which the count rates were extracted was carried out with a laser power that was not sufficient to distinguish between the background signal and the signal generated by very dim quantum dot clusters. The measurements on the luminescence decay were performed with an average laser power of $10^{-3} P_0$ in pulsed mode.

Discussion

Figure 5.3 shows that luminescence decay of the 655 nm quantum dots cannot be described entirely by a single or double exponential decay function, similar to the 605 nm quantum dots. The single exponent estimated characteristic decay time was found to be 31.9 ± 0.4 ns. If we zoom in on the first two decades of decay, we find that the SEDTF is not an accurate representation of the luminescence decay, even at the very start of the decay, as can be observed in Figure 5.4. From the same figure we conclude that the DEDTF performs better and can be used as a reasonable approximation of the first two decades of luminescence decay of bright 655 nm quantum dot clusters. The characteristic decay time of the fast and major energy-transition was found to be 14.5 ± 0.2 ns with a relative magnitude

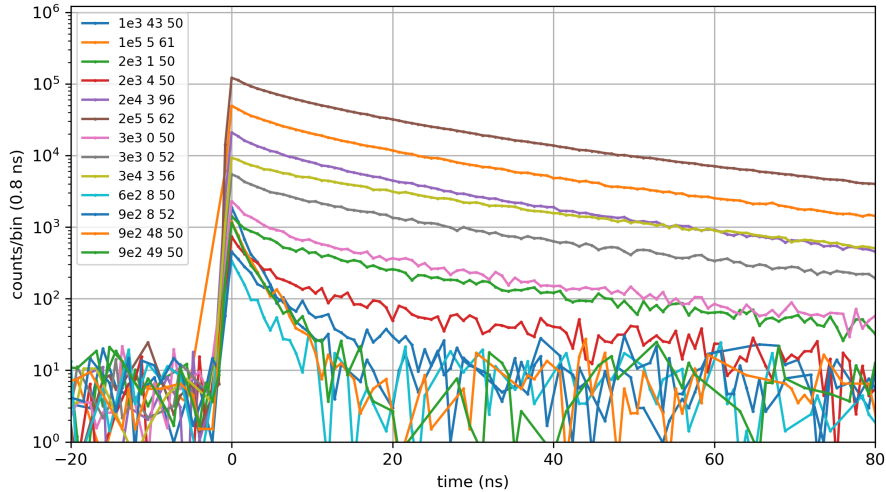


Figure 5.7: Comparison of luminescence decay of different quantum dot clusters. The position-dependent count rates are indicated in the legend.

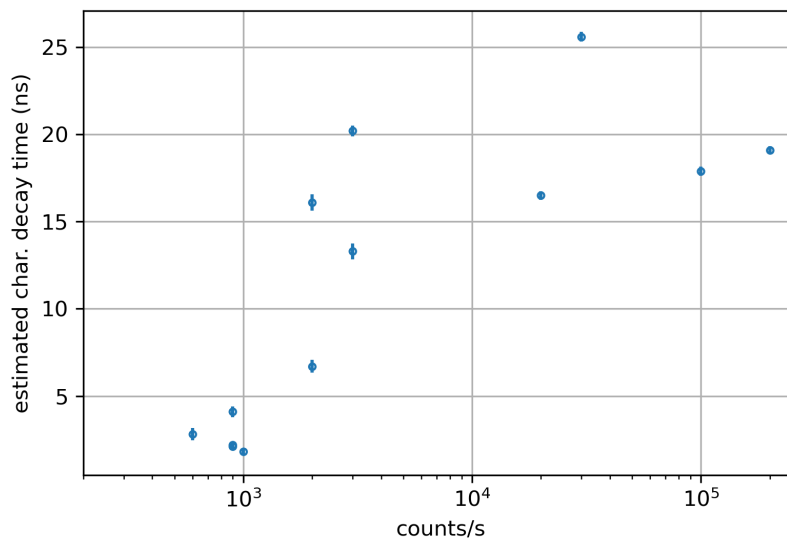


Figure 5.8: Scatter plot of the estimated single exponential characteristic decay times of the measurements shown in Figure 5.7 over the position-dependent count rate from a spatial scan.

of 0.6 and a characteristic decay time of 44.3 ± 0.3 for the slower energy-

transition with a relative magnitude of 0.4.

From Figure 5.4 we conclude that the SEDTF cannot be used to accurately describe the first two decades of luminescence decay of 655 nm quantum dots.

From Figure 5.5 we conclude that the estimated decay rate does not depend on the laser power, nor the received signal strength by the SPCM. We discovered that the optimization of the SEDTF on the luminescence decay of the bright quantum dot cluster depends on the range that the fitting is applied. A fit of the SEDTF over the first two decades of decay resulted in an estimated characteristic decay time τ of 31.9 ns, whereas a fit over solely the first decade of decay resulted in the estimation $\tau = 26.3$. As the low power measurement only shows approximately one decade of decay before the background signal takes over, we are convinced the fit restricted to the first decade of decay is more reliable when comparing the high and low power measurement.

When we applied the DEDTF fit to the first decade of decay of the low power measurement, we found characteristic decay times $\tau_1 = 0.01$ ns with a relative magnitude of 0.1 and $\tau_2 = 26.7 \pm 0.8$ ns with a relative magnitude of 0.9. As the major estimated characteristic decay time is very comparable to the SEDTF decay time and has high relative magnitude, we conclude that the luminescence decay of the 655 nm quantum dot cluster can be described with a SEDTF during the first decade of decay at very low laser powers. It is unclear what the underlying cause is for this difference between the low and high laser power measurement.

From Figure 5.8 we conclude that the 655 nm quantum dots have widely differing characteristic decay times, ranging from $\tau = 2$ ns up to $\tau = 26$ ns for the SEDTF fits on the first decade of decay. As was already stated for the 605 nm quantum dots, brighter quantum dot clusters generally show longer characteristic decay times. Figure 5.8 reinforces this observation. We find a positive correlation between the fluorescence signal strength from a spatial scan and the estimated characteristic decay time using the SEDTF on the first decade of decay. It remains unclear what causes larger quantum dot clusters to have a slower luminescence decay.

5.4 Bleaching and blinking

Results

Figure 5.9 shows the gradual decrease of the fluorescence signal of a quantum dot cluster on *Sample 12* (the medium density sample) when exposed to a continuous wave laser power of P_0 . The corresponding measurement had a duration of 120 s and was performed with a laser power of P_0 . The time tagged photon events were distributed over 1 s bins. The first ~ 5 s were measured with the laser turned off and show the background signal, resulting in the first plateau with a value of ~ 450 counts per 1 s bin. The next ~ 5 s were measured at an empty spot on the sample, measuring the fluorescence signal generated by the sample glass, resulting in the second plateau with a value of ~ 1300 counts per 1 s bin. After the second plateau, the laser is focused on the quantum dot cluster. An initial signal strength of $2 \cdot 10^3$ counts/s was found. Over the course of 110 s, the fluorescence signal strength gradually drops to $1.8 \cdot 10^3$ counts/s, resulting in a bleaching rate of $\sim 0.1\%$ per second.

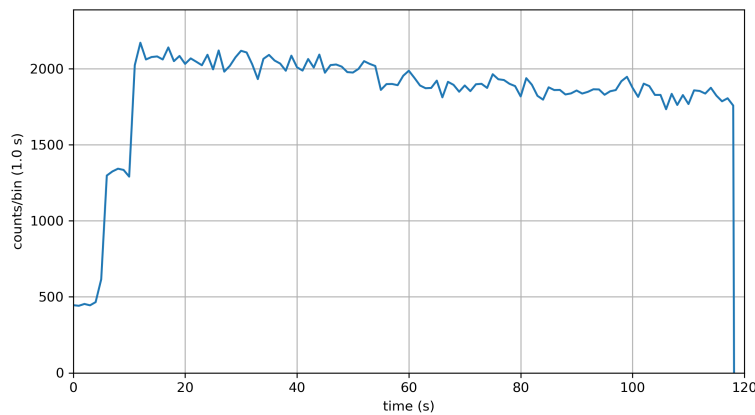


Figure 5.9: Time resolved dynamics of a quantum dot cluster on *Sample 12*. The first plateau is the dark count rate of the new SPCM. The second plateau is the background fluorescence of the sample glass. The apparent gradual bleaching of 2 counts/s^2 is surprising, as it suggests that a single quantum dot contributes very little to the total signal strength of the quantum dot cluster during this measurement. We conclude that the laser beam was not focused optimally on the quantum dot cluster during the measurement, resulting in a sub-optimal signal strength.

Figure 5.10 shows the time resolved dynamics of a fluorescence source

on *Sample 10* (also shown on the right of Figure 5.1). The figure consists of four concatenated, 120 s TTTR measurements of photon events that are distributed over 0.1 s bins. The measurements were carried out with a laser power P_0 . Each measurement starts with ~ 5 s of background signal, resulting in the four signal drops that can be seen in the figure. Again, the plateaus have a value of approximately 50-60 counts/bin, or 500-600 counts/s, corresponding roughly to the dark count rate of the 'new' SPCM. Each plateau is followed by ~ 5 s of recording of the fluorescence signal from the sample glass, with a value of approximately 70 counts/bin, or 700 counts/s, corresponding with the background fluorescence signal that can be observed on the right of Figure 5.1. After around 60 s, fluorescence signal that surpassed the background fluorescence signal was observed, increasing the measured signal with a value of approximately 30-40 counts/bin or ~ 300 -400 counts/s. This is in agreement with the fluorescence signal value for the local variable of the right spatial scan of Figure 5.1. This fluorescence signal showed up and disappeared periodically, with periods of darkness in the order of 10-50 s. After the second 120 s measurement, the fluorescence signal of a 1000 counts/s was not observed again, as can be seen in the figure.

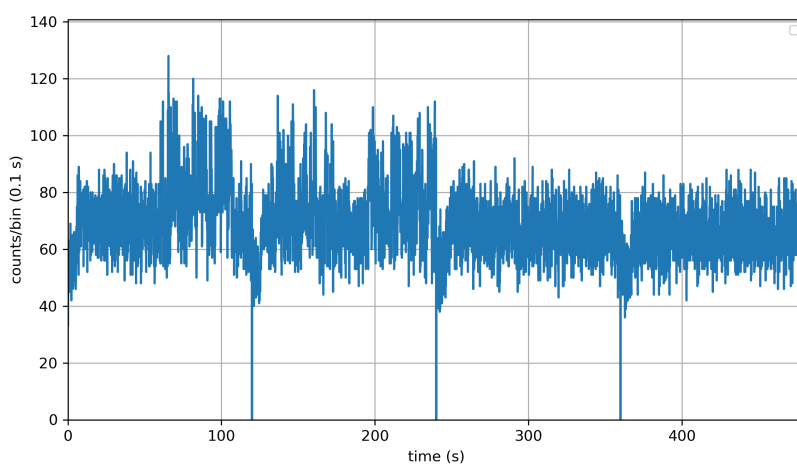


Figure 5.10: Concatenation of the four 120s time trace measurements of the quantum dot on the right of Figure 5.1. Each plateau signifies the start of a new 120s measurement. Each plateau is followed by ~ 5 s of sample glass fluorescence.

Discussion

From the time trace experiments we conclude that the 655 nm quantum dots also show both blinking and bleaching behaviour, which should be taken into account during other measurements.

Quantized bleaching can be observed in Figure 5.10. After approximately 200 seconds of laser exposure with power P_0 , the fluorescence signal of the quantum dot(s) disappeared and did not reappear during the following experiments. We conclude that the quantum dot(s) have bleached as a consequence of prolonged high power laser exposure.

In addition to the quantized bleaching, Figure 5.10 shows blinking behaviour. We observed periods of approximately 10 - 50 s of fluorescence darkness. When the fluorescence signal reappears after a period of darkness, it appears to return to the original signal strength of ~ 300 -400 counts/s, showing only two states.

The observation of quantized bleaching combined with the apparent two-state blinking behaviour convinces us that the quantum dot shown on the right of Figure 5.1 is a single quantum dot, producing ~ 300 detected fluorescence photons per second at a laser power of P_0 .

5.5 Conclusions

Similar to the 605 nm quantum dots, the 655 nm quantum dots have widely differing fluorescence characteristics. In the cross sectional scans we have observed fluorescent sources with differing signal strength up to a factor $2 \cdot 10^4$ and comparable FWHM sizes of $\sim 1.2 - 2 \mu\text{m}$. We conclude that the actual spatial resolution has remained constant between the measurements on the 605 nm and 655 nm quantum dots. In addition, we conclude that the 655 nm quantum dots also have a high tendency of clustering and even super clustering and that these clusters have a size much smaller than the spatial resolution of the experimental setup. In contrast to the observed clustering, it is plausible that a single quantum dot has also been observed on the right of Figure 5.1.

The first two decades of luminescence decay of bright 655 nm quantum dot clusters cannot be described accurately by a fitted SEDTF. However, measurements on the same quantum dot cluster with a far lower laser power show luminescence decay that can be described by a SEDTF much better. The estimated characteristic decay time did not differ between these measurements. It is unclear what causes the difference in the shape of the luminescence decay measured with high and low laser power.

A fit of the DEDTF on the luminescence decay of bright quantum dot clusters proved to be more successful, again suggesting that other, slower energy transitions play a prominent role in the luminescence decay of 655 nm quantum dot clusters.

The estimated characteristic decay time of the 655 nm quantum dots differs widely and ranges between 2 ns and 26 ns when fitted with the SEDTF on the first decade of decay. This difference in characteristic decay time can be observed in Figure 5.7. From Figure 5.8 we conclude that the fluorescence signal strength from a spatial scan and the estimated characteristic decay time are positively correlated.

Similar to the 605 nm quantum dots, the effects of bleaching and blinking were observed for the 655 nm quantum dots and should be taken into account when conducting research. Gradual bleaching was observed and is shown in Figure 5.9, where the fluorescence signal drops with a rate of 2 counts/s². In comparison, Figure 5.10 shows instantaneous bleaching with a signal drop of 300 counts/s. We conclude that the laser was not optimally focused during the experiment shown in Figure 5.9. In addition to the instantaneous signal drop, we observed two-level blinking behaviour. The combination of these two observations makes it very plausible that the matching fluorescence source is a single quantum dot. With this assumption, we conclude that single 655 nm quantum dots have a signal strength of ~ 300 counts/s when exposed to a laser power of P_0 .

Concluding discussion

Chapter 4 and 5 discuss the results of research on the fluorescence properties of 605 nm and 655 nm colloidal quantum dots respectively. Both types of quantum dots were investigated using the same methods. This chapter aims to compare the conclusions of both chapters and to give an overall conclusion on the general fluorescence characteristics of both types of quantum dots.

In general, spatial scans show a high tendency of clustering for both the high density samples and the low density samples. We determined the spatial resolution of the confocal setup by analyzing the FWHM of local maxima of fluorescence signal of different magnitudes. We found that the FWHM does not depend on the signal strength of the local maxima and conclude that the size of the imaged quantum dot clusters is much smaller than the spatial resolution of the setup. Both type of quantum dots show high diversity in cluster brightness, with signal strength differing up to a factor 5000 between clusters on the high density samples and clusters on the low density samples. If we assume that the measured fluorescence intensity of a cluster is proportional to the number of quantum dots in the given cluster, we find high variation in the number of quantum dots that are located in the observed clusters. The background fluorescence signal of $\sim 800 - 1200$ counts/s generated by the sample glass was a limiting factor in the detection of single quantum dots. A single quantum dot has been detected in the case of 655 nm quantum dots, with an estimated signal strength of ~ 300 counts/s when exposed to a laser power of $P_0 \approx 1$ mW.

The luminescence decay of both types quantum dots was found to differ widely and to be correlated to the number of quantum dots in a quantum dot cluster. Characteristic decay times have been estimated by fitting a single exponent decay template function to the data. The estimated de-

cay times differed between 6 ns and 20 ns for the 605 nm quantum dots and 2 ns and 26 ns for the 655 nm quantum dots. Both types of quantum dots show exponential decay that cannot entirely be described by a single exponent decay function. Only the first two decades of decay of bright 605 nm quantum dot clusters can be approximated by the single exponent decay template function, whereas even the first decade of decay of bright 655 nm quantum dot clusters cannot be approximated in this way. However, when bright 655 nm quantum dot clusters were measured with a very low laser power, the luminescence decay could be described by a single exponent decay function. In contrast to the shape of the decay, the estimated characteristic decay time remained constant. It remains unclear why the shape of the luminescent decay changes with the provided laser power.

A double exponent decay function proved to be a better approximation of the observed behaviour, but is only able to reasonably describe the first two decades of decay for both types of quantum dots. We conclude that both types of quantum dots show other, slower energy transitions that play a non-negligible role in the luminescence decay.

The effect of blinking and bleaching have been observed for the two types of quantum dots. Both 605 nm and 655 nm quantum dot clusters on the high density samples show a gradual decrease of fluorescence over time when exposed to a maximum laser power of P_0 . This effect of bleaching has also been observed to occur in a more quantized way, where the signal appears to decrease in steps of 250 counts/s in the case of 605 nm quantum dots. In the case of the 655 nm quantum dots, a sudden and permanent drop of fluorescence signal of 300 counts/s to the background fluorescence level was observed. Based on the similarity of these drops in fluorescence signal, we make the tentative assumption that single quantum dots have a fluorescence signal strength of ~ 300 counts/s in this setup when exposed to a laser power of $P_0 \approx 1$ mW.

The effect of blinking was only encountered when investigating dim quantum dot clusters. These small ensembles of quantum dots showed sudden temporary periods of lower or non-existent fluorescence signal on time scales of 0.1 seconds up to tens of seconds. This blinking behaviour can also be observed indirectly in the spatial scans, where sources of fluorescence seem to be stretched in the x-direction.

In conclusion, we do not recommend the use of these quantum dots for similar or follow-up research, as the fluorescence properties differ widely and because the quantum dots are very susceptible to the effects of bleaching and blinking.

Appendix

7.1 Python measurement UI

With the use of the TKinter module for python, a UI class was developed to facilitate the measurement process. Figures 7.1, 7.2 and 7.3 show the different windows of the UI. Figure 7.3 shows the main window of the UI.

On the left of the main window spatial scans can be executed. The fields 'start x pos' and 'start y pos' take values between 0 and 100 and set the starting coordinates of the spatial scan. The field 'distance' is used to set the scanning distance for both the x and y direction (be cautious with this input value, as the PI-E517 has a maximum range of $\sim 100 \mu\text{m}$). The 'steps' field controls the amount of measurements steps taken to traverse the scanning distance. The amount of data points therefore is steps^2 . The buttons below are self-explanatory.

To the right of the scanning menu, we find a menu that is loosely related to saturation measurement. The three upper fields can be used to set the position of the PI-E517 by entering the coordinates and pressing the 'set piezo position' button on the right of the window. The buttons below are self-explanatory. One important button is the 'set min attenuator voltage' button and its matching input field right below. This can be used to set the maximum laser power when performing any other measurement. A higher voltage means a lower laser power, with a voltage ranging from 0 to 5 volts.

To the right of the saturation menu, a bleaching measurement menu is found. These function were rarely used and need more testing.

All the way to the right the general options can be found. The different functions are explained in Table 7.1.

button	function
create new experiment	opens the experiment naming prompt and creates a new experiment directory. All measurements performed after this action will be stored in this new directory.
exit program	sets the laser power to 0 (in order to prevent bleaching) and terminates the program.
call custom function	executes a custom function which can be added to the python ode.
set piezo position	sets the position of the PI-E517 to the coordinates entered in the coordinates field above the 'start saturation' button.
get current piezo position	prints the current position of the PI-E517 to the console.
get current count rate	measures and prints the photon count rate at the current position.
max laser power	sets the attenuator voltage to the value set by the 'set min attenuator voltage' button (default value is 0).
min laser power	sets the attenuator voltage to 5 volts (turns off the laser).
get current laser power	estimates the power on the sample based on the voltage reading of the photodiode (see Table 3.1.) and prints it to the console.
optimize z position	scans the z-position of the PI-E517 on the correct x and y position and returns a graph with the resulting count rate for each z-position. This function can be used to optimize the z-position of the setup (see Section 3.3).

Table 7.1: General functions of the UI menu.

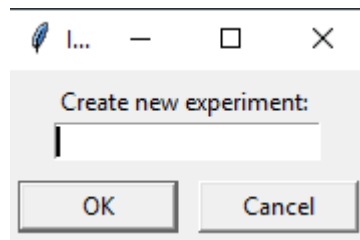


Figure 7.1: Starting screen of the measurement UI. The user can input the name of the experiment directory all the measurement data and figures will be stored in. The directory name will automatically be prefixed by a date tag.

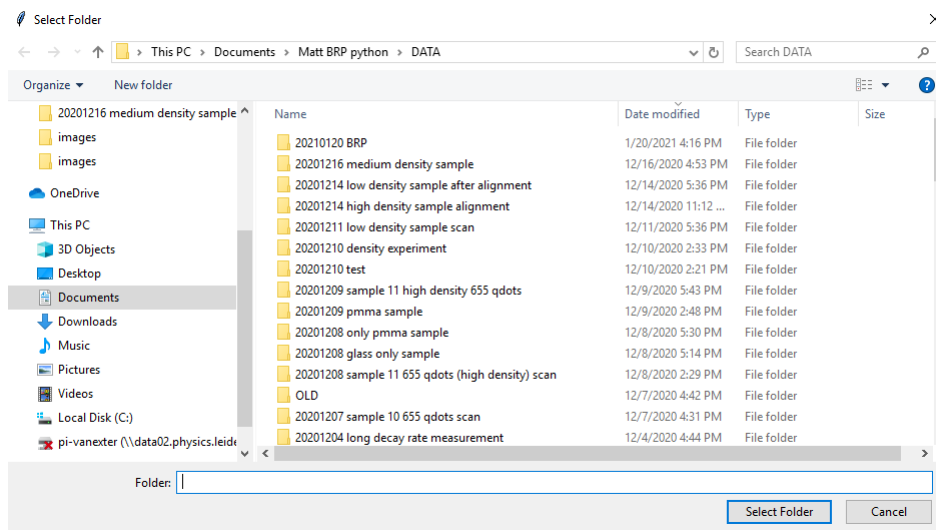


Figure 7.2: Second screen of the measurement UI. The user can choose where the experiment folder is stored.

The UI is by no means finished and bug-free, and should be tested and tweaked thoroughly before it can be used for follow-up research. The Python code is provided below.

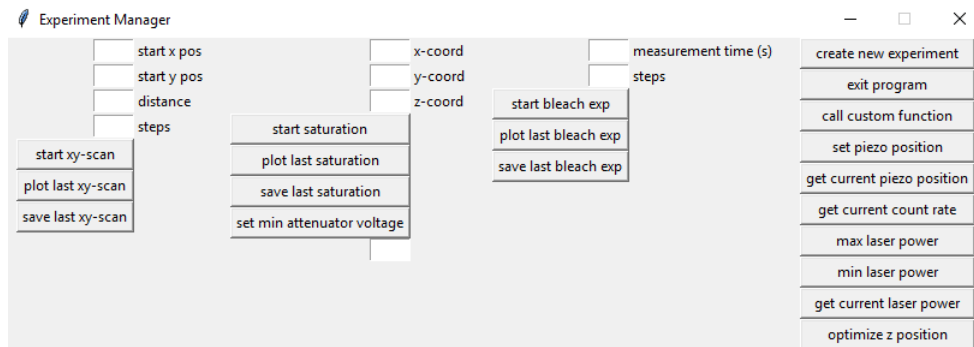


Figure 7.3: Main measurement UI.

```
# -*- coding: utf-8 -*-
# author: Matt van den Nieuwenhuijzen , mattvdnieuwhuijzen@gmail.com

import tkinter as tk
from tkinter import filedialog
from tkinter import simpledialog
from datetime import date
import os
import FLEXperiments as EXP
import time
import numpy as np
import matplotlib.pyplot as plt

# Function that assigns widgets to a window grid based on type
def SetWidgets(lst):
    index=0
    for i in lst:
        if isinstance(i, tk.Label):
            i.grid(row=index, column=1, sticky="w")
        elif isinstance(i, tk.Button):
            i.grid(row=index, column=0, sticky='nsew')
            index +=1
        else:
            i.grid(row=index, column=0, sticky='e')
            index +=1
    return

class ExpManager():
    """
    ExpManager creates a bridge between the UI and the different
    measurement classes and functions.
    """

    #TODO: print time indications
    #TODO: save files of z scan
    #TODO: power management with attenuator
    #TODO: fix size difference between scan plots

    def __init__(self):

        self.exp_folder = "C:/Users/lion/Documents/Matt_BRP_python/DATA/datadump"
```

```

self.Scan = EXP.XYScan(path=self.exp_folder)
self.Sat = EXP.Saturation()
self.Bleach = EXP.Bleaching()

self.CreateExpFolder()

self.polmax = 0
self.polmin = 5

self.PDzero = self.Sat.GetPower()
self.SetPolarizerMin()
return

def CreateExpFolder(self):
    """
    Asks the user for a path where the data of this session should be saved.
    """
    input_window = tk.Tk()
    input_window.withdraw()
    exp_name = simpledialog.askstring("Input", "Create new experiment:",
                                     parent=input_window)

    folder_picker = tk.Tk()
    folder_picker.withdraw()
    file_path = filedialog.askdirectory()

    today = date.today().strftime("%Y%m%d")

    self.exp_folder = "{}/{}-{}".format(file_path, today, exp_name)
    self.Scan.path = self.exp_folder

    if (not os.path.exists(self.exp_folder)): os.mkdir(self.exp_folder)
    input_window.destroy()
    folder_picker.destroy()
    return

def SetPolAngle(self):
    value = max(min(float(ent_polangle.get()), 5), 0)
    self.polmax = value
    print("attenuator voltage set to {} V".format(value))
    return

def GetPower(self):
    print("laser power is {} watts".format(self.Sat.GetPower()-self.PDzero))

def OptimizeZ(self):
    #todo reset z position
    self.SetPolarizerMax()
    self.Scan.ZScan(self.exp_folder)
    self.SetPolarizerMin()

def SaveScan(self):
    self.Scan.SaveData(self.exp_folder)
    return

def PlotScan(self):

```

```

self.Scan.PlotData()
self.Scan.PlotData(lower_lim=100, upper_lim=3000, linear=True)
self.Scan.PlotData(lower_lim=100, upper_lim=1000, linear=True)
self.Scan.PlotData(lower_lim=None, upper_lim=None, linear=True)
return

def MakeScan(self):
    self.SetPolarizerMax()
    startpos = [float(ent_ystart.get()), float(ent_xstart.get())]
    distance = float(ent_scandistance.get())
    steps = int(ent_scansteps.get())

    print("starting_scan")
    self.GetPower()

    self.Scan.Scan(startpos, distance, steps)
    self.SetPolarizerMin()
    self.PlotScan()
    return

def SetPosition(self):
    x = ent_xcoord.get()
    y = ent_ycoord.get()
    z = ent_zcoord.get()
    self.Scan.SetXY(y,x)
    self.Scan.SetZ(z)
    print("position_set!")
    return

def GetPosition(self):
    position = self.Scan.ReturnCurrentPiezoPosition()
    print("current_position:")
    print(position)
    return position

def GetCountRate(self):
    self.SetPolarizerMax()
    time.sleep(2)
    print("count_rate_at_current_position")
    print(self.Scan.ReturnCountRate(autoDisable=True))
    self.SetPolarizerMin()
    return

def MeasureSaturation(self):
    self.SetPolarizerMax()
    self.Sat.MeasureSaturation(self.exp_folder)
    self.SetPolarizerMin()

def SetPolarizerMax(self):
    self.Sat.SetPolarizerAngle(self.polmax)

def SetPolarizerMin(self):
    self.Sat.SetPolarizerAngle(self.polmin)

def BleachExp(self):

```

```

        self.SetPolarizerMax()
        time = float(ent_bleachtime.get())
        steps = int(ent_bleachsteps.get())
        self.Bleach.MeasureBleaching(time, steps, self.GetPosition())
        self.SetPolarizerMin()
        return

    def PlotBleach(self):
        self.Bleach.PlotData()
        return

    def SaveBleach(self):
        self.Bleach.SaveData()
        return

    def __del__(self):
        self.SetPolarizerMin()
        del self.Sat
        del self.Scan
        del self.Bleach
        window.destroy()

Experiment = ExpManager()

# =====
# TKINTER WINDOWS
# =====

window = tk.Tk()
window.title("Experiment_Manager")
window.resizable(width=False, height=False)

entryWidth = 5

# =====
# scan section
# =====
frame_scan = tk.Frame()

scan_items = [
    lbl_xstart := tk.Label(master=frame_scan, text="start_x_pos"),
    ent_xstart := tk.Entry(master=frame_scan, width=entryWidth),

    lbl_ystart := tk.Label(master=frame_scan, text="start_y_pos"),
    ent_ystart := tk.Entry(master=frame_scan, width=entryWidth),

    lbl_scandistance := tk.Label(master=frame_scan, text="distance"),
    ent_scandistance := tk.Entry(master=frame_scan, width=entryWidth),

    lbl_scansteps := tk.Label(master=frame_scan, text="steps"),
    ent_scansteps := tk.Entry(master=frame_scan, width=entryWidth),

    btn_scan := tk.Button(master=frame_scan, text="start_xy-scan", command=Experiment
        .MakeScan),

    btn_plotsc := tk.Button(master=frame_scan, text="plot_last_xy-scan", command=

```

```

        Experiment.PlotScan),
    btn_savesc := tk.Button(master=frame_scan, text="save_last_xy-scan", command=
        Experiment.SaveScan),
]

SetWidgets(scan_items)

frame_scan.grid(row=0, column=0, padx=10, sticky="nsew")

# =====
# saturation section
# =====
frame_saturation = tk.Frame()

sat_items = [

    lbl_xcoord := tk.Label(master=frame_saturation, text="x-coord"),
    ent_xcoord := tk.Entry(master=frame_saturation, width=entryWidth),

    lbl_ycoord := tk.Label(master=frame_saturation, text="y-coord"),
    ent_ycoord := tk.Entry(master=frame_saturation, width=entryWidth),

    lbl_zcoord := tk.Label(master=frame_saturation, text="z-coord"),
    ent_zcoord := tk.Entry(master=frame_saturation, width=entryWidth),

    btn_saturation := tk.Button(master=frame_saturation, text="start_saturation",
        command=Experiment.MeasureSaturation),

    btn_plotsat := tk.Button(master=frame_saturation, text="plot_last_saturation"),

    btn_savesat := tk.Button(master=frame_saturation, text="save_last_saturation"),

    btn_setangle := tk.Button(master=frame_saturation, text="set_min_attenuator_
        voltage", command=Experiment.SetPolAngle),
    ent_polangle := tk.Entry(master=frame_saturation, width=entryWidth)

]

SetWidgets(sat_items)

frame_saturation.grid(row=0, column=1, padx=10, sticky="nsew")

# =====
# bleaching section
# =====
frame_bleaching = tk.Frame()

bleach_items = [

    lbl_bleachtime := tk.Label(master=frame_bleaching, text="measurement_time_(s)"),
    ent_bleachtime := tk.Entry(master=frame_bleaching, width=entryWidth),

    lbl_bleachsteps := tk.Label(master=frame_bleaching, text="steps"),
    ent_bleachsteps := tk.Entry(master=frame_bleaching, width=entryWidth),

    btn_bleach := tk.Button(master=frame_bleaching, text="start_bleach_exp", command=

```

```

    Experiment.BleachExp),
    btn_plotbleach := tk.Button(master=frame_bleaching, text="plot_last_bleach_exp"),
    btn_savebleach := tk.Button(master=frame_bleaching, text="save_last_bleach_exp")
]

SetWidgets(bleach_items)

frame_bleaching.grid(row=0, column=2, padx=10, sticky="nsew")

# =====
# general options
# =====

frame_general = tk.Frame()

general_items = [
    btn_setpath := tk.Button(master=frame_general, text="create_new_experiment",
        command=Experiment.CreateExpFolder),
    btn_exit := tk.Button(master=frame_general, text="exit_program", command=
        Experiment._del_),
    btn_customfunction := tk.Button(master=frame_general, text="call_custom_function"
    ),

    btn_setposition := tk.Button(master=frame_general, text="set_piezo_position",
        command=Experiment.SetPosition),
    btn_getposition := tk.Button(master=frame_general, text="get_current_piezo_
        position", command=Experiment.GetPosition),
    btn_getcount := tk.Button(master=frame_general, text="get_current_count_rate",
        command=Experiment.GetCountRate),
    bnt_setpolmax := tk.Button(master=frame_general, text="max_laser_power", command=
        Experiment.SetPolarizerMax),
    bnt_setpolmin := tk.Button(master=frame_general, text="min_laser_power", command=
        Experiment.SetPolarizerMin),
    bnt_getpower := tk.Button(master=frame_general, text="get_current_laser_power",
        command=Experiment.GetPower),
    bnt_optimizez := tk.Button(master=frame_general, text="optimize_z_position",
        command=Experiment.OptimizeZ),
]

SetWidgets(general_items)

frame_general.grid(row=0, column=3, padx=10, sticky="nsew")

# Run the application
window.mainloop()

```

7.2 Python measurement classes

Below, the python code that was used to control the different devices from the experimental setup is shown. It consists of 3 classes. The XYScan class holds all actions and data related to spatial scanning of the fluorescence signal and can be used to set the position of the piezo controller with the functions SetXY and SetZ. The Bleaching class holds all actions and data related to a bleaching measurement. This class was rarely used, as a time trace with the use of the th260 software proved to be a more useful method of observing bleaching. Finally, the Saturation class holds all actions and data related to saturation measurements. This class can also be used to set and measure the current laser power with the functions SetPolarizerAngle (this name is deprecated since the laser power controlling polarizer was later replaced by a voltage controlled optical attenuator) and GetPower.

```
# -*- coding: utf-8 -*-
# author: Matt van den Nieuwenhuijzen , mattvdnieuwhuijzen@gmail.com

from PIPiezo import E517
from th260_master import th260 as TH
import numpy as np
import time
import math
import matplotlib.pyplot as plt
import thorlabs_appt as apt

import nidaqmx as dx
from nidaqmx.constants import Edge
from nidaqmx.constants import AcquisitionType
from nidaqmx import stream_writers

import Analytics as AL

# Minimal timedelay between consecutive measurements of a device
TimeHarpSleep = 0.15
piezoSleep = 0.1

# Deadtime of the spc
DEADTIME = 40e-9

# Upper and lower limit of count rate range of the th260 API
TH_upper=np.log10(5e5)
TH_lower=np.log10(8e1)

#returns a timestamp
def TimeStamp():
    return str(int(time.time()))

#corrects the count rate based on deadtime
def CountCorrection(countrate):
    return (1/(1-DEADTIME*countrate))*countrate

# =====
```

```

# XYSCAN
# =====

class XYScan():
    """
    XYScan manages all actions that are related to scans of the sample.
    """

    # TODO: SPC dead-time count rate correction
    # TODO: fix limits of plots
    # TODO: save values of z scan

    def __init__(self, path):
        self.Piezo = E517.E517()

        self.TimeHarp = TH.TH260(TH.get_available_devices()[0])

        self.xCoords = []
        self.yCoords = []
        self.counts = []

        self.maxima = []

        self.timeStamp = 0

        self.zcoord = 0

        self.startpos = 0
        self.distance = 100
        self.steps = 10

        self.Figure = None
        self.Ax = None

        # If true more information is printed during the experiments
        self.debug = True
        self.path = path

        print("XYScan initialised")
        return

    def EnableTH(self):
        self.TimeHarp.openDevice()
        self.TimeHarp.initialize(settings={'mode': 2})

    def DebugMode(self, mode):
        #Toggle debug mode
        if (mode): self.debug = True
        else: self.debug = False

    def ZScan(self, path):
        # TODO: fix first point of measurement?

        current_position = self.ReturnCurrentPiezoPosition()
        self.EnableTH()

        # the first measurement is always off for some reason...
        _ = self.ReturnCountRate()

        positions = np.arange(0, 100, 0.5)
        counts = np.empty(positions.shape)

```

```

for i in range(len(positions)):
    self.SetZ(positions[i])
    counts[i] = self.ReturnCountRate()
    print("z={}_with_{}".format(positions[i], counts[i]))

optimal = positions[np.argmax(counts)]
print("optimal_z_for_this_position_is: {},_with_a_value_of_{}".format(
    optimal, max(counts)))

fig, ax = plt.subplots()

ax.plot(positions, counts, marker='o')
ax.set_title("z_scan_at_{}".format(current_position))
ax.set_xlabel("z_position_(micrometer)")
ax.set_ylabel("counts/s")
ax.grid(True)

plt.show()

savepath = "{}/{}_zscan".format(path, TimeStamp(), current_position)
fig.savefig("{}_png".format(savepath), dpi=300)
np.savetxt("{}_z_positions.csv".format(savepath), positions, delimiter=",",
    "")
np.savetxt("{}_counts.csv".format(savepath), counts, delimiter=",")

self.TimeHarp.closeDevice()

def Scan(self, startpos, distance, steps):
    """
    Scan a section with area distance^2 starting from startpos, using 'steps'
    amount of steps. The th260 api is used to measure the count rate at each
    position. The result of the scan is stored in a local variable matrix
    of the class and can be used by other functions after the scan is
    finished.
    """

    tiles=steps**2
    counter=0
    percent=1

    print("estimated_duration_of_operation: {}_minutes".format((tiles*0.3)
        /60))

    self.EnableTH()

    self.startpos = startpos
    self.distance = distance
    self.steps = steps

    self.xCoords = np.arange(startpos[0], startpos[0]+distance, distance/
        steps)
    self.yCoords = np.arange(startpos[1], startpos[1]+distance, distance/
        steps)
    self.counts = np.empty([steps, steps])

    for i in range(steps):
        for j in range(steps):
            self.SetXY(self.xCoords[i], self.yCoords[j])
            self.counts[i,j] = self.ReturnCountRate()
            counter+=1
            if(int(math.floor((counter/tiles)*100)) >= percent):
                print("{}%".format(percent))

```

```

        percent+=1

    print("")
    print("Scan completed!")
    # self.maxima = AL.FindLocalMaxima(self.counts)
    # self.maxima[:,0] = self.startpos[0]+self.maxima*(self.distance/self.steps)
    # self.maxima[:,1] = self.startpos[1]+self.maxima*(self.distance/self.steps)

    # print("local maxima found at: ")
    # print(self.maxima)

    self.timeStamp = TimeStamp()

    self.TimeHarp.closeDevice()
    return

def SetXY(self, xCoord, yCoord):
    """
    Sets the x and y position of the PI controller.
    """
    self.Piezo.set_position(x=yCoord, y=None, z=xCoord)
    time.sleep(piezoSleep)
    return

def SetZ(self, zCoord):
    """
    Set the z position of the PI controller. Increasing the z will
    increase the distance between the sample and the objective.
    (this needs to be checked!)
    """
    self.Piezo.set_position(x=None, y=zCoord, z=None)
    time.sleep(piezoSleep)
    self.zcoord = zCoord
    return

def ReturnCurrentPiezoPosition(self):
    """
    Asks the PI controller for its current positions and returns the result.
    """
    posDic = self.Piezo.get_position()
    return [posDic['X'], posDic['Y'], posDic['Z']]

def PlotData(self, lower_lim=TH.lower, upper_lim=TH.upper, linear=False,
             color=plt.cm.jet):
    """
    Plot the results of the last scan using a logarithmic heat map.
    """
    if(self.xCoords.size == 0 or self.yCoords.size == 0 or self.counts.size
       == 0):
        print("No data available")
        return

    self.Figure, self.Ax = plt.subplots()

```

```

self.Figure.set_size_inches(9, 5, forward=True)

if (linear):
    counts = self.counts
    tag = 'lin'
else:
    counts = np.log10(self.counts)
    tag = 'log10'

im = self.Ax.pcolor(self.yCoords, self.xCoords, counts, vmin=lower_lim,
                    vmax=upper_lim, shading='nearest', cmap=color)
self.Ax.set_xlabel("x_position (micrometer)")
self.Ax.set_ylabel("y_position (micrometer)")
self.Ax.grid(True, color="black", lw=0.5)
cb = self.Figure.colorbar(im, ax=self.Ax)
cb.set_label("log(counts/s)", rotation=270, labelpad=15)
self.Ax.set_aspect("equal")
self.Ax.set_title("counts/s_per_position , z={}".format(self.
                ReturnCurrentPiezoPosition()[1]))
plt.show()

savepath = "{}/{}".format(self.path, self.timeStamp)

self.Figure.savefig("{}_xy-scan_{}_{}_{}.png".format(savepath, tag,
                lower_lim, upper_lim), dpi=300)
return

def SaveData(self, path):
    """
    Save the data of the last scan to a given path in csv format.
    """

    if (self.Figure == None): self.PlotData()
    savepath = "{}/{}".format(path, self.timeStamp)
    np.savetxt("{}_x.csv".format(savepath), self.xCoords, delimiter=",")
    np.savetxt("{}_y.csv".format(savepath), self.yCoords, delimiter=",")
    np.savetxt("{}_counts.csv".format(savepath), self.counts, delimiter=",")
    return

def ReturnCountRate(self, autoDisable=False):
    """
    Return the measured count rate of the TH at the current position.
    """

    if (autoDisable): self.EnableTH()
    counts = self.TimeHarp.getCountRate(channel=0)
    time.sleep(TimeHarpSleep)
    if (autoDisable): self.TimeHarp.closeDevice()
    return counts

def __del__(self):
    self.TimeHarp.closeDevice()

# =====
# BLEACHING
# =====

```

```

class Bleaching():
    """
    Bleaching manages all actions that are related to a bleaching experiment.
    """

    # TODO: enhance plotting

    def __init__(self):
        self.TimeHarp = TH.TH260(TH.get_available_devices()[0])

        self.timeArray = []
        self.counts = []

        self.Figure = None
        self.Ax = None

        self.Position = []
        return

    def __EnableTH(self):
        self.TimeHarp.openDevice()
        self.TimeHarp.initialize(settings={'mode': 2})
        return

    def ReturnCountRate(self, autoDisable=False):
        if (autoDisable): self.__EnableTH()
        counts = self.TimeHarp.getCountRate(channel=0)
        time.sleep(TimeHarpSleep)
        if (autoDisable): self.TimeHarp.closeDevice()
        return counts

    def MeasureBleaching(self, seconds, steps, position):
        """
        For a duration of x seconds, a y amount of times the count rate is
        measured at a given position. If bleaching is occurring, a decrease in
        count rate is expected to be seen over time. The result is stored in
        a local variable for later use.
        """

        self.__EnableTH()
        self.Position = position

        self.timeArray = np.arange(0, seconds, seconds/steps)
        self.counts = np.empty(steps)

        for i in range(steps):
            self.counts[i] = self.ReturnCountRate()
            time.sleep(seconds/steps)
            print("{}_seconds_to_go".format(seconds - i*(seconds/steps)))

        self.PlotData()
        self.TimeHarp.closeDevice()
        return

    def PlotData(self):
        """
        Plot the results of the last bleaching experiment.
        """

```

```

self.Figure, self.Ax = plt.subplots()
im = self.Ax.plot(self.timeArray, self.counts, 'r+')
self.Ax.set_xlabel("time_(s)")
self.Ax.set_ylabel("counts")
self.Ax.set_title("counts_over_time_at_{}".format(self.Position))
plt.show()
return

def SaveData(self, path):
    if (self.Figure == None): self.PlotData()
    savepath = "{}_{}_{}".format(path, Timestamp(), self.Position)
    self.Figure.savefig("{}_bleaching.png".format(savepath), dpi=300)
    np.savetxt("{}_time.csv".format(savepath), self.timeArray, delimiter=",")
    np.savetxt("{}_counts.csv".format(savepath), self.counts, delimiter=",")
    return

# =====
# SATURATION
# =====

class Saturation():

    # TODO: accurate voltage to power conversion
    # TODO: implement saturation measurement
    # TODO: limit sample exposition to high power

    def __init__(self):
        self.TimeHarp = TH.TH260(TH.get_available_devices()[0])

        self.powers = None
        self.counts = None

    def EnableTH(self):
        self.TimeHarp.openDevice()
        self.TimeHarp.initialize(settings={'mode': 2})
        return

    def ReturnCountRate(self, autoDisable=False):
        if (autoDisable): self._EnableTH()
        counts = self.TimeHarp.getCountRate(channel=0)
        time.sleep(TimeHarpSleep)
        if (autoDisable): self.TimeHarp.closeDevice()
        return counts

    def MeasureSaturation(self, path, steps=100):
        self.EnableTH()

        voltages = np.linspace(0, 5, steps)
        self.power = np.empty(voltages.shape)
        self.counts = np.empty(voltages.shape)

        for i in range(len(voltages)):
            self.SetPolarizerAngle(voltages[i])
            self.power[i] = self.GetPower()
            self.counts[i] = self.ReturnCountRate()

```

```

self.TimeHarp.closeDevice()

fig, ax = plt.subplots()
ax.plot(self.power, self.counts, marker='o', markersize=0.2)
ax.set_xlabel("estimated_power_at_sample_(miliwatts)")
ax.set_ylabel("counts/s")
ax.set_title("counts/s vs. power_at_sample")
ax.grid(True)
plt.show()

savepath = "{}/{}_saturation_curve".format(path, TimeStamp())
fig.savefig("{}_png".format(savepath), dpi=300)
np.savetxt("{}_power.csv".format(savepath), self.power, delimiter=",")
np.savetxt("{}_counts.csv".format(savepath), self.counts, delimiter=",")

return

def MeasurePowerCurve(self):
    positions = np.linspace(5, 0, 100)
    power = np.empty(positions.shape)

    self.SetPolarizerAngle(positions[0])
    time.sleep(0.05)

    for i in range(len(positions)):
        print("current_voltage_{}_V".format(positions[i]))
        self.SetPolarizerAngle(positions[i])
        power[i] = self.GetPower()

    self.SetPolarizerAngle(5)
    plt.plot(positions, power, marker='o', markersize=0.2)
    plt.xlabel("voltage_on_attenuator_(V)")
    plt.ylabel("estimated_power_at_sample_(miliwatts)")
    plt.title("beam_power_vs_attenuator_voltage")
    plt.grid(True)
    plt.show()
    return

def SetPolarizerAngle(self, voltage):
    v = min(max(0, voltage), 5)

    daqOut = dx.Task()
    daqOut.ao_channels.add_ao_voltage_chan('Dev1/ao0')
    writer = stream_writers.AnalogSingleChannelWriter(daqOut.out_stream,
        auto_start=True)

    writer.write_one_sample(v)

    daqOut.stop()
    daqOut.close()

    return

def GetPower(self, avg_only=True):
    """
    Returns the power measured at the diode in miliwatts.
    """

    sample_rate=20000
    measure_time=0.2

```

```
wedge_percentage=0.0594
respons=0.5
resistance=2e5

daqIn = dx.Task()

daqIn.ai_channels.add_ai_voltage_chan('Dev1/ai0')

daqIn.timing.cfg_samp_clk_timing(sample_rate, source="", active_edge=Edge
    .RISING, sample_mode=AcquisitionType.FINITE, samps_per_chan = int(
    sample_rate * measure_time))
data = daqIn.read(int(sample_rate*measure_time))
daqIn.stop()
daqIn.close()

data= np.asarray(data)/(wedge_percentage*respons*resistance)

if (avg_only): return np.average(data)*1000
else: return [np.average(data), np.std(data)]*1000

def __del__(self):
    self.TimeHarp.closeDevice()
```

Bibliography

- [1] Debasis Bera et al. "Quantum Dots and Their Multimodal Applications: A Review". In: *Materials* 3.4 (2010), pp. 2260–2345. ISSN: 1996-1944. DOI: 10.3390/ma3042260. URL: <https://www.mdpi.com/1996-1944/3/4/2260>.
- [2] Perkin Elmer. *Photodiode Modules Receiver for Analytical Molecular Applications*. URL: https://www.perkinelmer.com/PDFS/downloads/dts_photodiodemodulesreceiverforanalyticalmolecularapplications.pdf. (accessed: 20.01.2021).
- [3] Mark Fox and Juha Javanainen. "Quantum Optics: An Introduction". In: *Physics Today - PHYS TODAY* 60 (Sept. 2007). DOI: 10.1063/1.2784691.
- [4] Nikolai Gaponik et al. "Progress in the Light Emission of Colloidal Semiconductor Nanocrystals". In: *SMALL* 6.13 (2010), 1364–1378. DOI: {10.1002/smll.200902006}.
- [5] X Michalet et al. "Properties of fluorescent semiconductor nanocrystals and their application to biological labeling". In: *SINGLE MOLECULES* 2.4 (2001), 261–276. DOI: {10.1002/1438-5171(200112)2:4<261::AID-SIM0261>3.0.CO;2-P}.
- [6] Mohammad Jafar Molaei. "A review on nanostructured carbon quantum dots and their applications in biotechnology, sensors, and chemiluminescence". In: *Talanta* 196 (2019), pp. 456–478. ISSN: 0039-9140. DOI: <https://doi.org/10.1016/j.talanta.2018.12.042>. URL: <http://www.sciencedirect.com/science/article/pii/S0039914018313092>.

- [7] ThermoFisher Scientific. *Molecular probes the handbook: qdot nanocrystal technology*. URL: <https://www.thermofisher.com/nl/en/home/references/molecular-probes-the-handbook/ultrasensitive-detection-technology/qdot-nanocrystal-technology.html>. (accessed: 20.01.2021).
- [8] Andrew M. Smith and Shuming Nie. "Next-generation quantum dots". In: *NATURE BIOTECHNOLOGY* 27.8 (2009), 732–733. DOI: {10.1038/nbt0809-732}.
- [9] Wilfried G.J.H.M. van Sark et al. "Blueing, bleaching, and blinking of single CdSe/ZnS quantum dots". English. In: *ChemPhysChem* 3.10 (Oct. 2002), pp. 871–879. ISSN: 1439-4235. DOI: 10.1002/1439-7641(20021018)3:10<871::AID-CPHC871>3.0.CO;2-T.
- [10] Xiaoyong Wang et al. "Non-blinking semiconductor nanocrystals (Retraction of vol 459, pg 686, 2009)". In: *NATURE* 527.7579 (2015). DOI: {10.1038/nature15745}.
- [11] Xiaoyong Wang et al. "RETRACTED: Non-blinking semiconductor nanocrystals (Retracted article. See vol. 527, 2015)". In: *NATURE* 459.7247 (2009), 686–689. DOI: {10.1038/nature08072}.